Analysis of Geothermal Resources in Three Texas Counties

Joseph Batir and Maria Richards

SMU Geothermal Laboratory

Roy M. Huffington Department of Earth Sciences

Southern Methodist University

Dallas, Texas 75275-0395

October 16, 2020

Research results for Task 5 of the Project:

The Geothermal Entrepreneurship Organization (Geo) Accelerating Technology Transfer, Testing and Adoption of Cutting-Edge Extreme Environment Drilling

The University of Texas at Austin

DOE-GTO Prime Award: DE-EE0008971

Subaward number: UTA19-001356

Project Investigators: Jamie Beard and Robert Metcalfe

Table of Contents

Abstract

This project updated the geothermal resources beneath our oil and gas fields, as part of the research for the Texas GEO project. This report "Analysis of Geothermal Resources in Three Texas Counties" October 2020, improves on previous mapping of the Texas resources for the counties of Crockett (West Texas), Jackson (central Gulf Coast) and Webb (South Texas). Through additional bottom-hole temperatures (BHT) from oil and gas wells drilled in the late 1990s to 2019, the number of well sites increased from 532 to 5,410 in total for these counties. Therefore, most of the surface area within each county has at least one well within a 10 x10 km area to provide gridding stability from well data representation. The project improved the methodology to calculate formation temperatures from 3.5 km (11,500 ft) to 10 km (32,800 ft), included thermal conductivity values more closely related to the actual county geological formations, and incorporated radiogenic heat production of formations and the related mapped depth to basement. The project results show deep temperatures as hotter than previously calculated, with temperatures of 150 °C possible for Webb County between depths of 2.6 – 5.1 kms, average 3.3 km; Jackson County between depths 3.0 – 5.4 kms, average 3.7 km; and Crockett County between depths of 2.7 – 8.0 kms, average 4.0 km. Temperatures are on average, 25 – 50 °C warmer at 3.5 km than previous studies. Based on the 150 °C temperature necessary for electrical production, 677 wells or 11.6 % of them have at least this temperature or higher. The biggest error bars (25%) are on the original BHT values because of an unknown related to the drilling fluid impact. The results reflect how increased drilling by the oil and gas industry contributes to improved understanding of these deeper reservoirs. This report focused on the heat, the next steps are to determine where fluids exist and movement of them within the formations. The oil and gas industry can be a significant resource for unlocking our ability as a nation to extract the geothermal heat resource. Improvements in the analysis of formation thermal conductivity, equilibrium temperatures, and assessment of the fluid flow capability within these formations are items that will aid in the accuracy of the calculation for heat extraction.

Reference: Batir, Joseph and Maria Richards, 2020, Analysis of Geothermal Resources in Three Texas Counties, Final Report for University of Texas at Austin DOE-GTO Prime Award: DE-EE0008971 project Texas Geothermal Entrepreneurship Organization (GEO). SMU Geothermal Laboratory, Dallas Texas 75275-0395. 60 p.

Introduction

This geothermal resource assessment examines in-depth the temperature, thermal conductivity, and radiogenic heat production within Crockett, Webb and Jackson Counties of Texas. From the improved data synthesis of these parameters for each sedimentary formation, the deep temperatures are calculated for depths from 3.5 km to 5 km and modeled from 5 km to 10 km below surface. The project builds on other Texas resource studies (Richards and Blackwell, 2012; Zafar and Cutright, 2014; Batir et al., 2018) and temperature-at-depth calculation methodology (Blackwell et al., 2006; Blackwell et al., 2011a; Stutz et al., 2015; Smith, 2016; Smith and Horowitz, 2017; Batir et al., 2018; Batir et al., 2020).

The results of this work are for the Texas Geothermal Entrepreneurship Organization (Geo) Project, to provide the Texas GEO Team with expanded knowledge for choosing test sites for their incubator projects. The results provide methods for future use by public and private organizations and/or individuals considering to use the geothermal resources in Texas. The three counties highlight the importance of detailed county mapping to provide the geothermal and oil and gas communities with increased overall understanding of expected depths necessary to drill to, in order to produce from formations within a temperature threshold.

The work described here does not include examination of geological items such as fluid flow, detailed fault mapping, and pressure regimes. Examination of these parameters is necessary as part of a play fairway geothermal resource evaluation to narrow-down exactly where to drill for a successful project. To increase the usefulness of these results, this report includes information on the limitations of the data, and where additional research and exploration will improve the success of finding and developing our geothermal resources.

Project Area Focus

The chosen project counties are based on the objective of expanding the temperature regime knowledge as an initial tool for geothermal development. Thus, the first goal is to refine the temperatures from 3.5 to 10 km of depth in areas with higher than background heat flow. The second goal is the inclusion of geologically significant oil and gas settings for both increase of drilling data and to provide our communities with knowledge of the related resources both co-mingled and below the oil and gas reservoirs. The third goal is to include areas with human activity and cities, who could be end-users of future produced electricity or direct-use applications. From these three goals, the focus of the research narrowed to Crockett, Webb, and Jackson Counties (Figure 1). All three counties include the following items: above continental average heat flow (based on the SMU Geothermal Laboratory U.S Geothermal Map (Blackwell et al., 2011b)), high data density across each county in the National Geothermal Data System (NGDS), high activity of oil and gas field(s), colocation with large population centers, and at least one of the following mineral rights ownership: University of Texas - University Lands, Texas General Lands Office, and/or U.S. Department of Defense (DOD).

County Overview

Through the initial review of the surface and deep parameters, Crockett, Webb, and Jackson Counties meet the required criteria for deep (> 1 km, 3,280 ft) well data, detailed formation descriptions, and temperature data. The counties also included multiple surface end-use stakeholders.

The following descriptions are of the three counties studied (Figure 1).

1) **Crockett County** - This county has a large and disperse dataset to improve the geothermal map and a large tract of University of Texas Lands. Crockett County currently has limited active oil

and gas drilling rigs, providing an opportunity for positive geothermal potential to increase oil and gas industry interest, especially on the University Lands property.

2) **Jackson County** - This county is in the center of the onshore Gulf Coastal Plain, and part of the geopressured resources. The county is to the southeast of the main Eagle Ford Shale trend. This location is of interest because of the coastal geologic trends and potential to add to the geothermal resource understanding for areas outside of the Eagle Ford activity. The potential stakeholders are the town of Victoria and towns along Lavaca Bay.
3) **Webb County** - This county contains densely dispersed oil and gas well data. Webb County is also on the edge of a heat flow transition zone, which is refined through the additional data. This evaluation provides the opportunity to refine heat flow around the large population center of Laredo. It is expected for the geothermal resources to continue into Zapata County, to the south, also with high heat flow based on the resource mapping by Blackwell et al. (2011). Webb and Zapata Counties are on the Mexican International border; therefore, developers may qualify for unique funding opportunities.

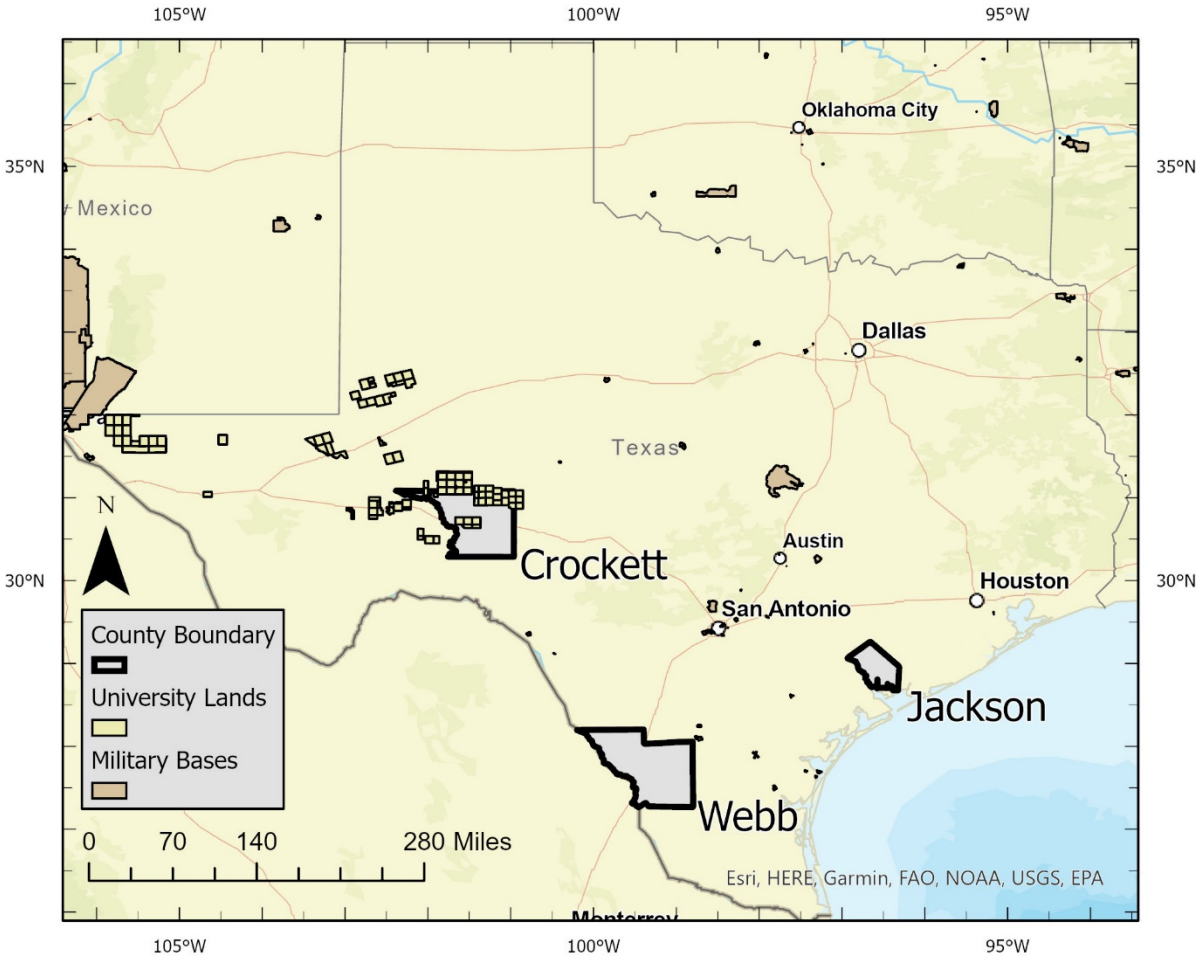

Figure 1. Location of the chosen counties in relation to University Lands, Military Bases, and major cities.

Our initial review of Texas counties identified other counties for future detailed temperature studies to help promote the Texas Energy Industry's expansion into geothermal energy. The following is a list of counties and the advantages each one provides.

1) **El Paso and Hudspeth Counties** – New well data can improve the current mapping, which is based on only ~10 data points for the region. Ft. Bliss explored for shallow geothermal resources (albeit unsuccessfully) that could be expanded to deep (10 km) depth.
2) **Andrews County** - Large amount of acreage on University Lands with sufficient well data coverage to improve the geothermal resource knowledge base. The heat flow is currently mapped at ~50 mW/m², therefore, this county may be reviewed for direct-use types of geothermal resource projects or overlapping opportunities with solar power.
3) **Nueces County** - There are additional wells drilled since the last 2011 Blackwell et al. maps. Being close to Webb County allows researchers the ability to examine the extent of geological variations and associated changes in temperature regimes. Corpus Christi and multiple military properties provide additional incentive for end users to gain from the research.
4) **Brazoria, Galveston, Chambers, Jefferson Counties** (West and East of Galveston Bay) –An unfunded UT Austin-BEG machine learning proposal is aimed at comparing a current geothermal resource evaluation (such as this project) with a machine learning evaluation of the volumes of research completed in the 1980s- 90s on geopressured-geothermal resources. Funding that project could build on our methods and advance the Houston - Galveston corridor in resource evaluation.
5) **DeWitt, Goliad, Victoria Counties** – These counties are of interest because of the potential stakeholders in Victoria and the military infrastructure in Goliad. There was a DOE Geothermal Technologies Office funded gas field to geothermal conversion project in Goliad. It provided important details highlighting how too much gas can cool the borehole fluids and become problematic for geothermal electrical development. This area is of geologic interest, including the geologic transition zone of the Sligo and Stewart City shelf margins as well as the San Marcos Arch. These geologic transitions make this area more complicated, requiring more in-depth studies. The population and potential-end users in Victoria, the infrastructure around Lavaca Bay, and as a continuation of the work performed in Jackson County make it worthwhile.

There is interest to explore in-depth the counties (Bexar to McLennan) between San Antonio and Waco (western side of I-35) (Figure 2) because of the density of population and the request for renewable energy sources. These counties have few oil and gas wells, for acquiring the necessary temperatures for calculating heat flow and to model deep temperatures-at-depth. The surface geology is bedrock, rather than sedimentary. An analysis of this region requires different data collection methods, including using public and private water wells and geothermal heat pump boreholes (Rybach, 2020) to build a temperature data set.

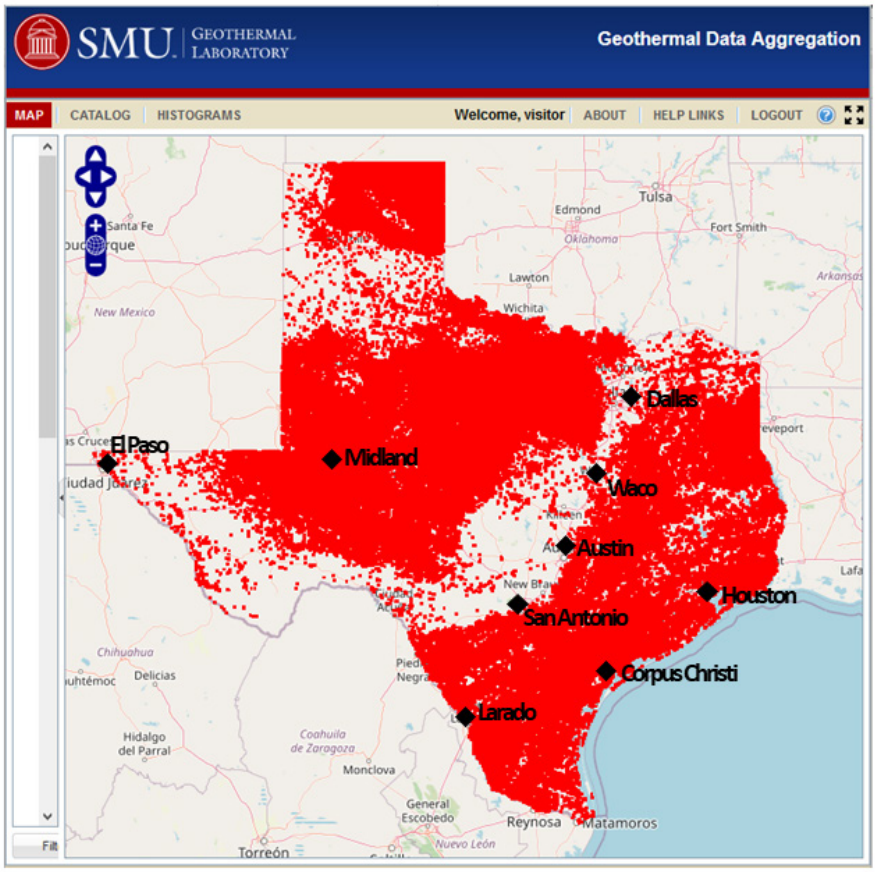

Figure 2. Map of Texas well data locations currently in the SMU Node of the National Geothermal Data System (NGDS).

Methodology

The collection, processing, and synthesizing of the data are discussed in this section. These parameters build the foundation to calculate the site heat flow. The updated methods and models are refined for this project to increase the resolution of temperatures to 10 km depth on a surface grid of 10 km by 10 km.

The thermal model to calculate heat flow and temperatures at various depths is the simplified steady-state one dimensional heat diffusion equation with additional radiogenic heat production. The methodology uses an input of a thermal conductivity model and geothermal gradient data for each site to first calculate heat flow, which then becomes the foundation to calculate the deep formation temperatures. Next, the combined heat flow, thermal conductivity model, and detailed sedimentary section and basement properties are the inputs to calculate temperature to as deep as 10 km (Smith, 2016; Smith and Horowitz, 2017).

A literature review refined the sedimentary formations and thicknesses in order to build a county to sub-county level stratigraphy. These stratigraphic columns allow for site-specific thermal conductivity models. From the review process, we developed new basement thickness models for Webb and Jackson Counties. The recent geophysical study of Agrawal et al. (2015) is also used to confirm the thickness of the upper crust for radiogenic heat production. These changes improve the accuracy and resolution of the resulting temperatures and prospective geothermal areas.

Temperature Data

The temperature data came from the National Geothermal Data System (NGDS) using the SMU Node (NGDS, 2020). The files downloaded are the Borehole Temperature Observation data set and Heat Flow data set following their respective content model formatting. These two data sets include many parameters from oil and gas wells, in addition to geothermal wells (NGDS, 2020). For temperature data, the minimum requirement is a surface latitude and longitude, well temperature and depth of that temperature (Figure 3). The available downhole temperature data in the counties are from oil and gas well bottom-hole temperature (BHT).

Examination of the Borehole and Heat Flow files found overlapping surface location sites, therefore duplicates of site temperature - depth data were removed. The Borehole Temperature Observation file includes all the Heat Flow file sites, plus it contains many additional well sites. For consistency in calculating heat flow between the new sites and existing data, the raw temperatures from the Borehole data set are used as the temperature data input for this study.

There is a significant increase in data density across all three counties (Figure 3, Table 1), thereby increasing heat flow and the temperature-at-depth spatial resolution for mapping the deeper (1 – 10 km) depths. Jackson County has the fewest well sites in this study. The current data are evenly distributed throughout the county and also vertically to depths of 5 km (Figure 3) strengthening the results. Crockett County data density increases significantly in the southern portion of the county, with less infilling of data in the northern half. Webb County also significantly increases in the total number of sites, with data coverage following the general trends of previous sites.

The Borehole temperatures are extracted from oil and gas well log headers and these values are expected to be disturbed from drilling fluids, therefore, the Harrison correction is applied to all temperature values based on their depth, as previously done by Blackwell et al. (2011). This correction is designed to increase the BHT for depths below 1 km (3,280 ft) as drilling fluid is expected to have cooled the formation fluids in the borehole and the well has not yet returned to an *in situ* setting before measurement takes place. The raw temperatures increase approximately from 0 °C at 1 km to a maximum of 19.1 °C at 3.8 km. Beyond 3.8 km all temperatures have an increase of 19.1 °C. In examining the percent increase of the raw temperatures between 2 – 4.5 km for each county, it highlights the overall temperatures of that county, i.e., the warmer the raw temperatures the smaller percent increase. Note, in working with the Borehole Temperature Observation file, this cut-off of the Harrison Correction at 19.1 °C is not the method used for the BEG:IGOR data, rather those data points have a continuous increasing temperature correction to the deepest depths. It is our expectation that the deeper the well is drilled, the less time spent with drilling fluids at those deeper depths and more time between drilling and temperature measurement. These differences allow for a more representative raw temperature value of the *in-situ* setting, therefore requiring less of a correction. The temperature values plotted in Figure 3 are the Harrison corrected temperatures, not raw data from Borehole Temperature Observation file.

As a well surface location has one bottom-hole temperature (BHT) for every drilling interval, it is possible to have more than one temperature-depth pair per well site (Table 1). In the Borehole data set it is rare to have multiple well BHTs per site making it difficult to calculate interval temperature gradients. Consequently, this study uses the average ground surface temperature (Gass, 1982) as the top temperature for each BHT to determine the well gradient. It becomes possible to have more than one gradient per well. There were 374 sites with two temperature-depth measurements and 8 sites with three or more temperature-depth measurements. Spot checks on some of these data sites show similar interval gradients with the general trend of the surrounding well sites.

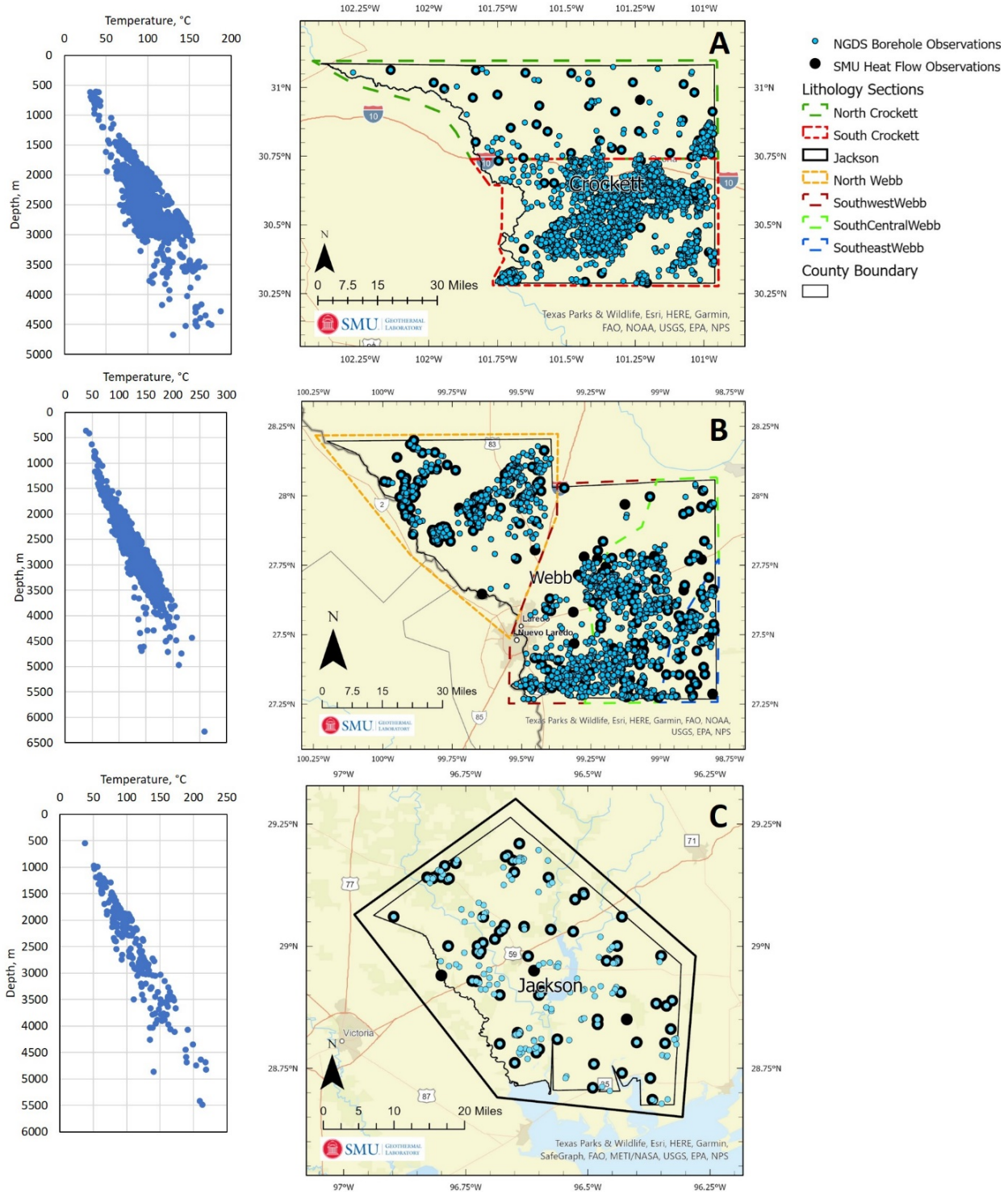

Figure 3. Temperature-depth plots of Harrison corrected BHT (left) and data density maps (right) for Crockett, Webb, and Jackson Counties. SMU Heat Flow data from 2011 temperature-at-depth maps (black circles) and Borehole Temperature Observation sites as teal dots. Note, data points outside of two standard deviations are removed from these temperature-depth plots and data location maps.

Table 1. Data points examined by county.

County	2011 Map Number of Well Sites	2020 Initial Number of Well Sites	Number of Temperatures (BHT)	% of Raw BHT Correction Increase	Calculated Heat Flow Outliers Removed	Final Calculated Heat Flow Point Count
Crockett	65	3487	3733	17	230	3503
Jackson	80	215	232	14.6	4	228
Webb	387	1708	2229	13.3	142	2087

Thermal Conductivity Determination

The parameter of thermal conductivity varies based on the rock minerals, formation age, and geological setting (e.g., pressure, surrounding fluids, structural setting). In Texas there are limited measured thermal conductivity values for the sediments below 1 km and none for the counties this project is studying. McKenna and Sharp (1998a) measured thermal conductivity of the Wilcox and Frio formations at three localities in the South Texas portion of the Gulf Coast Basin. Their results show how thermal conductivities of Wilcox and Frio sandstones range from 2.06 to 5.03 $Wm^{-1}K^{-1}$ based on changes in the porosity range from 2.4 to 29.6%, with lower porosity trending with higher thermal conductivity. The other factor on the conductivity was how clean the sandstone samples were of clays/silts. Although formations are named, e.g., Eagle Ford Shale, Wilcox Sandstone, etc., even these can include layers of sandstone, shale, silts, etc. McKenna and Sharp (1998a) highlights the importance of location specific measurements for site-specific analysis for commercial projects.

This project incorporates the thermal conductivity values used in the past with additional refinement. We built on the Blackwell et al. (2011) use of the Anadarko Basin formation values from core and cuttings measured on the divided bar (Gallardo and Blackwell, 1999; Carter et al., 1998), and the East Texas Deep Direct-Use study (Batir et al., 2018; Turchi et al., 2020), which incorporated the Pitman and Rowan (2012) values, assigned based on formation minerals, specifically percent sandstone, shale, silt, limestone, etc. for Louisiana transects of the formations across the state.

For the 2004 Geothermal Map of North America, Blackwell and Richards (2004) developed a thermal conductivity for BHTs from the AAPG Geothermal Survey locations (1994) based on an initial generalized model related to formation age and basin consolidation for each physiographic region. These values were increased for the Texas portion of the Blackwell et al. (2011) coordinating with other mapping work and thermal conductivity measurements in Mckenna and Sharp (1998b). For Jackson County these thermal conductivity values ranged from 1.89 to 1.97 $Wm^{-1}K^{-1}$, for Webb County from 1.96 to 2.11 $Wm^{-1}K^{-1}$, and Crockett County from 2.06 to 2.31 $Wm^{-1}K^{-1}$. All counties have a general trend of lower values toward the south and higher values to the north, thus moving away from the coast the sediments are more consolidated.

The work by Blackwell et al. (2011) outside of Texas improved the methodology to allow for a well-specific thermal conductivity with detailed stratigraphic columns from the sections of the AAPG COSUNA (1994) and related formation and/or lithology values in the Anadarko Basin. This improvement provided a method of incorporating the full geological column for each well and the resulting thermal conductivity assigned to that location is then associated with the formation depth and thickness weighted value of that specific location.

Pitman and Rowan (2012) did not measure core samples for thermal conductivity values, rather used a mixing matrix calculated value based on cross-sections in Louisiana. The model they used set thermal

conductivity values for conditions of 20 °C and 100 °C, with the values decreasing by approximately 8% from the 20 °C (higher values) to the 100 °C (lower values) (see Appendix A for details). Their worked focused on Gulf Coastal Plain formations that extend into Texas.

The thermal conductivity assignment follows the methods outlined above. Crockett County, containing older, more compressed formations is most similar with the measured values of the Anadarko Basin. Webb and Jackson Counties, mostly Gulf Coast sediments, are assigned values determined by Pitman and Rowan (2012). We assigned their 20 °C thermal conductivity value in the shallower lithology section and the 100 °C thermal conductivity value to formations that were likely to be hotter than 100 °C, using a 35 °C/km geotherm. Therefore, formations in the stratigraphic column deeper than 2.85 km are assigned the 100 °C thermal conductivity value. If the specific local stratigraphic unit/formation is not given a thermal conductivity value in Pitman and Rowan (2012), their closest stratigraphic equivalent age and lithology is used for the thermal conductivity value.

Once the generalized stratigraphic column is assigned thermal conductivities, it can then be scaled for well site differences in its formation thicknesses. This is accomplished by setting total column thickness equal to the depth to basement (a.k.a., total sediment thickness) and uniformly scaling the column to fit the local (shallower or deeper) sediment column thickness, all awhile conserving percent thickness of each formation. This site-specific stratigraphic column, with estimated thermal conductivity of each layer intersected, is next used to calculate a depth and thickness weighted thermal conductivity. The well column average of these weighted values is used for the heat flow and/or temperature-at-depth calculations (Blackwell et al., 2011; Horowitz et al., 2015; Smith, 2016; Smith and Horowitz, 2017). Each site is assigned a site averaged thermal conductivity value through this process. Tables of all assigned thermal conductivity values for each formation within each county and the developed detailed lithology sections are shown in Appendix A.

Details on Stratigraphy, Formation, Lithology

A review of oil and gas reservoir studies and public well data from the Texas Railroad Commission was performed to detail the lithology (physical characteristics) of the formations (rock layer with a consistent lithology) within the stratigraphic columns developed for each county or subsets in the county to align with regional geologic trends. This produced detailed stratigraphic columns composed of the regional formations that are then assigned to related well sites based on the given lithology section. This effort produced detailed thickness and rock type information within a subset of each stratigraphic column associated with hydrocarbon exploration research.

As the next step to construction of average formation thicknesses for each lithology model, public formation-top data were acquired where available from the company Welldatabase.com platform (Welldatabase, 2020). None of the lithology sections included the entire sedimentary package for the counties in this study. Often, the shallow formations are not reported, and the deepest sedimentary formations are not encountered in hydrocarbon exploration; therefore, the shallow and deep portions of the stratigraphic sections are not available. The Correlation of Stratigraphic Units of North America (COSUNA) data compilation (AAPG, 1994) is used to augment the stratigraphic column depth sections within the counties where no detailed study or public formation top information are accessible.

The COSUNA data compilation was a project sponsored by the American Association of Petroleum Geologists (AAPG) to correlate stratigraphic rock units across the nation and put the numerous basins into a regional and modern stratigraphic context (AAPG, 1994). In this way, the COSUNA data provides a single highly generalized stratigraphic column for a given basin or region from the basement all the way

to surface. A COSUNA section for a given region includes every possible formation that could be encountered and provides a thickness range for that formation. Often, the thickness range is large, e.g., 0 to 500 m. The rock type assigned to individual stratigraphic units are also generalized. Most stratigraphic units describe rock types, e.g., marly shale, or interbedded siltstone/sandstone/shale, etc., yet these do not include rock type percentages or descriptions on compositional changes with depth or region of the basin. Although not ideal, the COSUNA sections fill in data gaps to build complete lithology models designed for heat flow and temperature-at-depth calculations. When no other information is available, the COSUNA section rock type is used to assign a thermal conductivity and the average of the thickness range, for the given stratigraphic unit, is assigned. The individual lithology sections for each county, including the input data for each lithology section, are described below. See Appendix A for final columns with values used.

Crockett County

Hamlin (2009) produced a detailed lithology and depositional study of the Val Verde Basin's Lower Carboniferous Ozona Sandstone in Crockett County. The Ozona Sandstone study is the primary source of detailed lithology, examining the synorogenic Canyon sedimentary section of the Val Verde Basin. This section, because of the contemporaneous Ouachita thrust belt formation, contains the most variability of a given sedimentary section within the Val Verde Basin. The lithology changes within the Ozona depositional sequence from the Ozona arch in the northern part of Crockett County into the Val Verde Basin to the south. Thus, Crockett County is split into two general lithologies following changes in the Ozona depositional sequence (Figure 4): North Crockett on the Ozona arch and Central Basin Platform, and South Crockett, the portion of the Val Verde Basin containing deep water sediments on top of the Strawn Limestone (Hamlin, 2009). Lithology below the Strawn limestone are pre-orogeny and are assumed to be relatively consistent lithology and thickness across Crockett County. The sedimentary section overlying the Canyon depositional sequence is post-orogenic, therefore assumed to be a consistent thickness throughout Crockett County (AAPG, 1994; Hamlin, 2009). The formations that are not shown within the presented cross section are assigned rock types and thicknesses following the COSUNA lithology log for the Val Verde Basin, which are both above and below the Canyon depositional sequence (AAPG, 1994). For the complete detailed lithology section, see Appendix A.

Table 2. Data sources for heat flow calculations.

County	Temperature - Depth	Surface Temperature	Lithology Model	Thermal Conductivity
Crockett	NGDS (2020) – Borehole Observation Content Model	Gass (1982)	AAPG (1994) Hamlin (2009)	Carter et al. (1998) Gallardo and Blackwell (1999)
Jackson	NGDS (2020) – Borehole Observation Content Model	Gass (1982)	McDonnell et al. (2008) Hackley (2012) Kincade (2018)	Pitman and Rowan (2012)
Webb	NGDS (2020) – Borehole Observation Content Model	Gass (1982)	Baker (1995) Lambert (2008)	Pitman and Rowan (2012)

Table 3. Average values at county level from the SMU Blackwell et al. (2011) data set.

County	Heat Flow mW/m²	Heat Flow Std. Dev. mW/m²	Gradient °C/km	Gradient Std. Dev. °C/km	Assigned Well Site Thermal Cond. Variation $Wm^{-1}K^{-1}$	Rock Type Percentages SS/SH/LS/SED	Sedimentary Heat Production $\mu W/m^3$
Crockett	57	±13	25.0	±6.2	2.06 – 2.31	N/A	1
Jackson	59	±8	30.2	±4.0	1.89 – 1.97	N/A	1
Webb	67	±10	33.4	±4.8	1.96 – 2.11	N/A	1

Table 4. Average values for counties in this 2020 study and change as percent compared to the SMU (2011) values.

County	Heat Flow mW/m²	Heat Flow Std. Dev. mW/m²	Gradient °C/km	Gradient Std. Dev. °C/km	Depth Weighted Well Site Thermal Cond. Variation $Wm^{-1}K^{-1}$	Rock Type Percentages SS/SH/LS/SED*	Sedimentary Heat Production $\mu W/m^3$	Heat Flow Percent Increase	Gradient Percent Increase	Well Site Averaged Ther. Cond. Percent Increase
Crockett	77	±11	32.5	±4.6	2.11 – 3.40	5/22/31/42	0.8	35	30	4
Jackson	81	±11	34.1	±4.9	2.27 -2.55	30/22/0/48	1.4	37	13	20
Webb	93	±9	38.2	±3.5	2.22 – 2.49	21/11/18/50	1.0	39	14	20

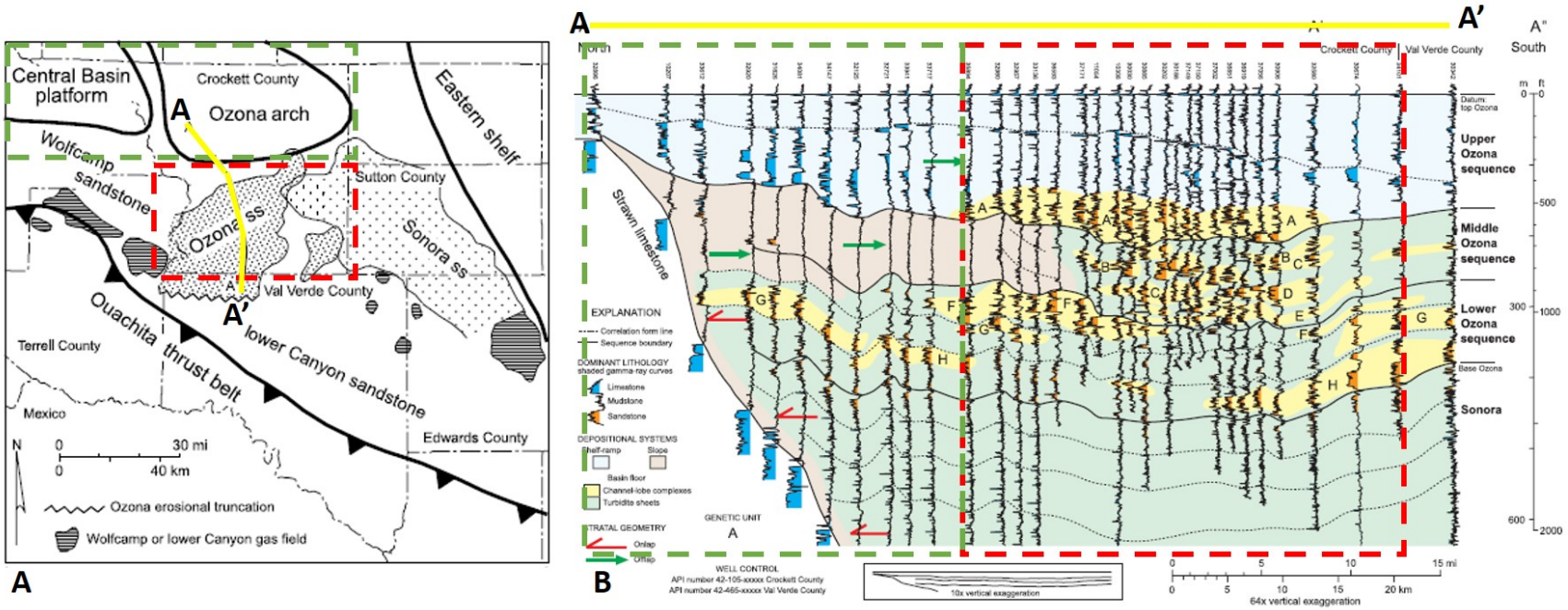

Figure 4. Crockett County Generalized Lithology Sections. (A) Map of Crockett County with regional geologic features. The North Crockett lithology section (green dashed box) coincides with the Ozona Arch and Central Basin Platform, while the South Crockett lithology section (red dashed box) is basinward with more traditional basin sediments. (B) High density gamma ray cross section A-A' from Hamlin (2009). North Crockett aligns approximately where the middle Ozona sequence goes from a slope depositional system to the basin floor depositional system.

Jackson County

Jackson County is on the present-day coastline of the Gulf of Mexico, on the eastern side of the San Marcos Arch, and within the Houston Embayment (Hackley, 2012). This county is south of the Cretaceous shelf edge and is crosscut by the Wilcox and Vicksburg fault zones (Kincade, 2018). Given the location, Jackson County was an offshore, deep abyssal plain until the Paleocene-Eocene time frame, with deposition of the Wilcox Formation being the oldest and deepest named section (Galloway, 2008). Undifferentiated, mostly overpressured shales underlie the Wilcox in the Jackson County region (McDonnell et al., 2008; Warwick, 2017). Most lithology is uniformly thick from surface to basement (Figure 5). The main exception is at the base of extensional growth faults located across the county. These growth faults produce an undulating contact between the Upper Eocene Jackson Group and the Late Oligocene Vicksburg Group, producing Jackson Group ridges estimated to be up to 1 km thick. While this is a significant variation, there is little difference within the thermal conductivity model between the formations at this depth. Pitman and Rowan (2012) present a thermal conductivity for the Jackson Group of 2.23 $Wm^{-1}K^{-1}$, and the Vicksburg Group is 2.3 $Wm^{-1}K^{-1}$, thus less than 5 % difference between them. While this is an important geologic boundary, there is little thermal difference introduced by the growth faults at the Oligocene-Eocene Boundary. Therefore, one generalized lithology section is utilized for Jackson County. The full sedimentary thickness is shown below in the cross section southeast of Jackson County, although the cross section shows stratigraphic packages by age and not formation. Individual formation information, where available, were combined with the available age cross section to produce a thickness and age correlated lithology section (McDonnell et al., 2008; Galloway, 2008; Hackley, 2012; Warwick, 2017; and Kincade, 2018). For the complete detailed lithology section, see Appendix A.

Webb County

Webb County is split into four different lithology sections, approximately following the Cretaceous continental shelf edge and surface geologic outcrops. The shelf edge and sediment influx that defined depositional environments, produced variations in the stratigraphic column as deposition location changed from shelfward (North Webb County) to basinward (South Webb County) during the Early to Middle Eocene (Lambert, 2004). South Webb County contains the Reklaw Formation, a marine shale, underlying the Bigford Formation, and a large section of the Queen City Sand, an interbedded clayey sandstone, which underlies the El Pico Clay. South Webb County is split into Southwest, Southcentral, and Southeast lithology sections that follow the geologic surface outcrops of the Yegua Formation, Jackson Group, and Frio Clay, respectively (Figure 6A and 6B). The uppermost lithologies are varied in thickness for the South Webb section based the surface geology and cross sections. North Webb County has minimal to no Reklaw Formation because of the position of the continental shelf, and contains only a minor section of the Queen City Sand, which thickens towards the southwest (Figure 6B). Baker (1995) produced less detailed cross sections, yet still show approximately consistent thickness from the Lower Cretaceous Pearsall Formation through present day (Figure 6C and 6D). Similarly, seismic lines outside of Webb County (Warwick, 2017) show that deeper sections can vary in thickness in the presence of growth faulting, highlighting that there may also be minor changes in thickness and variability. South Webb County contains growth faults, which introduce added uncertainty in thickness of the lithology section, but North Webb County contains less faulting and is assumed to contain relatively consistent formation thicknesses to basement. The Jurassic Norphlet Formation to the Lower Cretaceous Hosston Formation were not mapped by Lambert (2004) or Baker (1995) because they are deeper than any drilled wells. Details for these deeper formations are filled in using the COSUNA sections (AAPG, 1994). For the complete detailed lithology sections, see Appendix A.

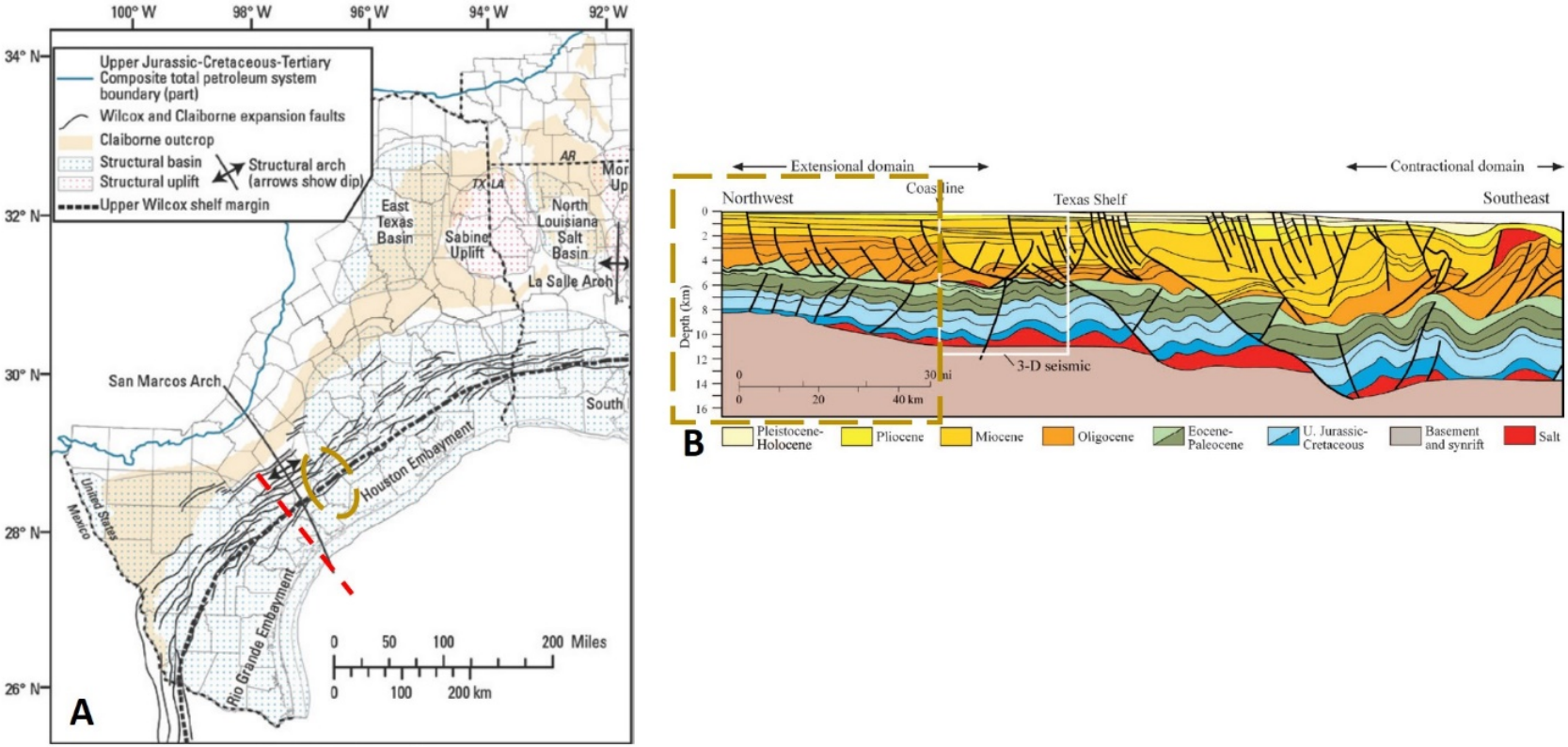

Figure 5. Jackson County Regional Tectonics. (A) The cross section highlighted as a red dashed line is shown in B. It is located on the western side of the San Marcos Arch, yet is considered applicable and equivalent to Jackson County (area within yellow dashed-line). (B) The cross section of the Texas Gulf Coast shows generally consistent stratigraphic age thicknesses from basement to surface. Modfied after McDonnell et al. (2008) and Hackley (2012).

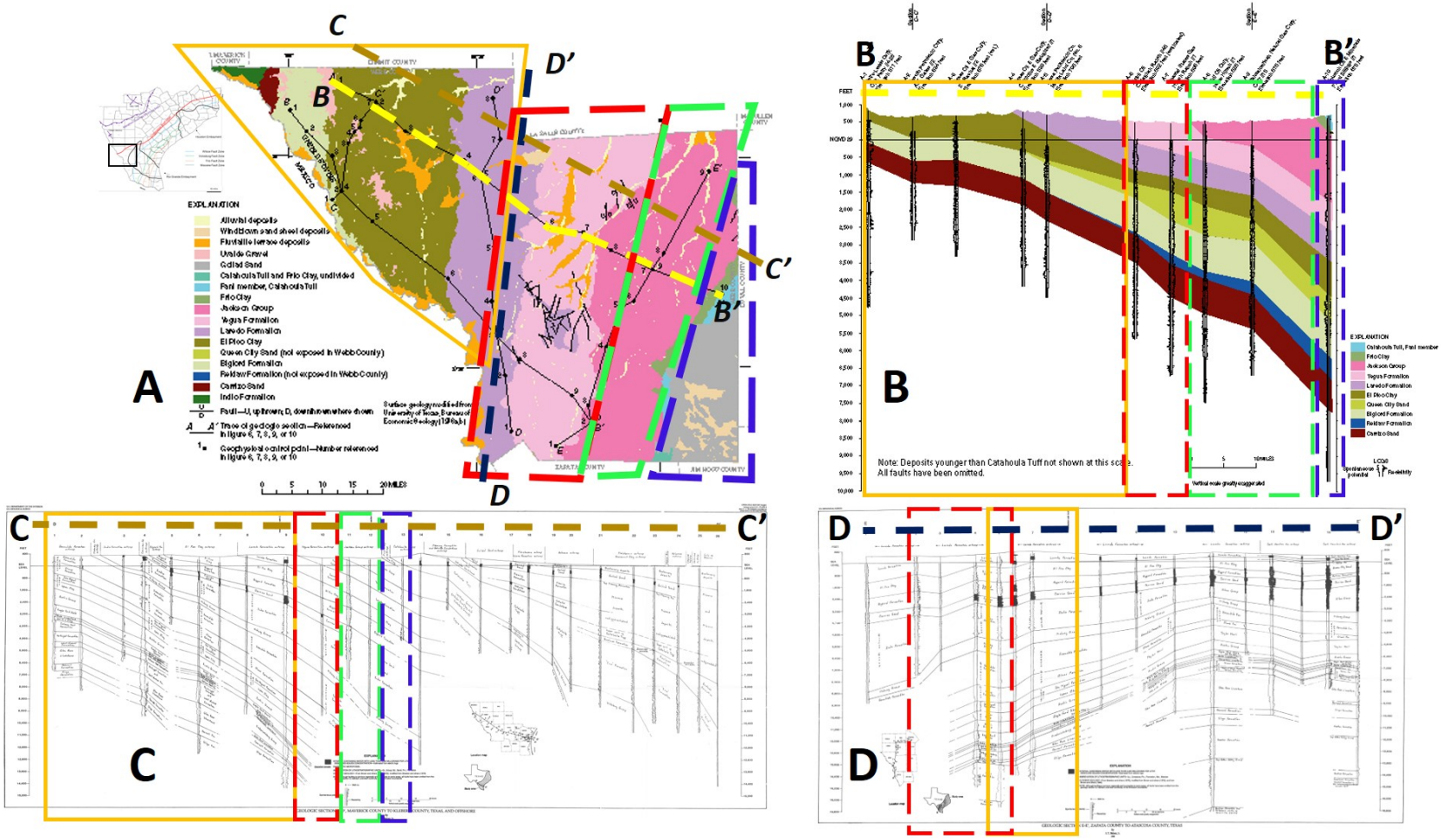

Figure 6. Generalized Stratigraphic Columns for Webb County (images modified from Lambert (2004) and Kincade (2018)). (A) Surface geology of Webb County and cross section positions. The golden triangle is the North Webb County lithologic section and the red, green, and blue dashed boxes are the Southwest, Southcentral, and Southeast Webb County lithologic sections, respectively. (B) Cross section B-B' showing the change in deposition of the Reklaw Formation (blue) and the Queen City Sand (greenish) moving from the Northwest to the Southeast, crossing the Cretaceous shelf margin. The onset of Reklaw deposition is the approximate location of the Cretaceous shelf margin and the separating point between North and South Webb County lithologic sections. (C) Cross section C-C' showing additional information for deposition of sediments down to the Sligo Formation. (D) Cross section D-D' showing that deposition and thickness is relatively consistent from south to north for deep formations.

Heat Flow Calculations

Heat flow is the product of the geothermal gradient multiplied by the thermal conductivity. Thus, the calculation requires two temperatures and associated depths to determine a geothermal gradient and an average weighted thermal conductivity value of the lithology within that depth interval. Heat flow measurements are assumed to be one dimensional with heat traveling upward out of the surface of the Earth, in a purely conductive thermal regime, and constant over the measurement distance. There is a decrease in heat flow with depth associated with older formations contributing less radiogenic heat production (~ 1 mW/m^2), although this heat flow loss is within the measurement margin of error.

The input data for this study are oil and gas BHT and the updated thermal conductivity stratigraphy sections. The temperature value error is up to 10%, the thermal conductivity value error is also up to 10%. There is an additional error associated with depth of the temperature measurement and the scaling of formation depths related to the thermal conductivity of ~ 5%. Most large errors in temperature and depth are removed initially in cleaning the data using two standard deviations from other nearby well sites. The combined error of heat flow values is considered 25%, which agrees with other related work (Richards and Blackwell, 2012).

The Heat Flow file is the preexisting SMU heat flow database for the study area and includes 532 data points with calculated heat flow from past studies work (Blackwell and Richards, 2004; Blackwell et al., 2011b). To include new data from the Borehole Temperature Observation file, for parameter consistency, all sites are calculated a heat flow for this study using the same method following the procedures outlined by Blackwell et al. (2006) and most recently discussed in Smith (2016). For the sites with multiple temperature-depth measurements, those heat flow values are averages for a site heat flow. From previous works listed above and Zafar and Cutright (2014), changes include inputs for the BHT corrections, the thermal conductivity values and methods, and the heat flow method for multi-temperatures. A comparison of final site heat flow to the most recent results (Blackwell et al., 2011b) are outlined in Tables 3 and 4. Note: A spreadsheet of all data analyzed is in the supplementary Excel file.

Heat Flow Data Analysis

Bullard Plot

Terrestrial heat flow values for each point are examined at the county lithology-section scale for outlier data using a Bullard plot (Figure 7). A Bullard plot is a graph plotting the site cumulative thermal resistance (1/thermal conductivity) for the stratigraphic column on the x-axis and the corrected temperature (BHT) on the y-axis. Plotted in this manner, the slope of a trend line is the average heat flow (times 1000) and b is the surface temperature. Data beyond two standard deviations of the trend line are considered outliers and not representative of the local conductive thermal regime. For example, in Figures 7 and 8, using this method, we removed the outlier data points (red circles) found in northeast Webb County before final heat flow mapping. Additionally, data points outside two standard deviations of site within a 1-km radius are also removed for mapping purposes. The final heat flow and temperature-at-depth data set for the 3 counties is 5818 data points out of the original 6194, with 376 data points excluded from the final mapping dataset (Table 1).

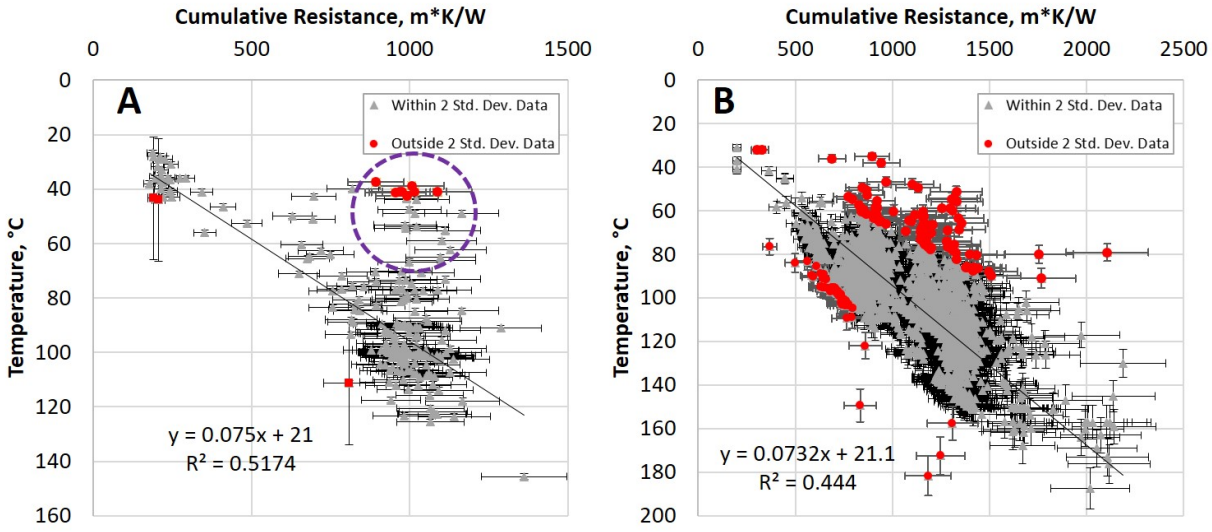

Figure 7. Example Bullard plots from Crockett County. (A) North Crockett Bullard plot, which shows outlier data (red dots). Purple dashed circle data discussed in Figure 8. (B) South Crocket Bullard plot of preliminary data with a generally consistent trend. Data outside two standard deviations (red circles) were excluded from the heat flow and temperature-at-depth modeling.

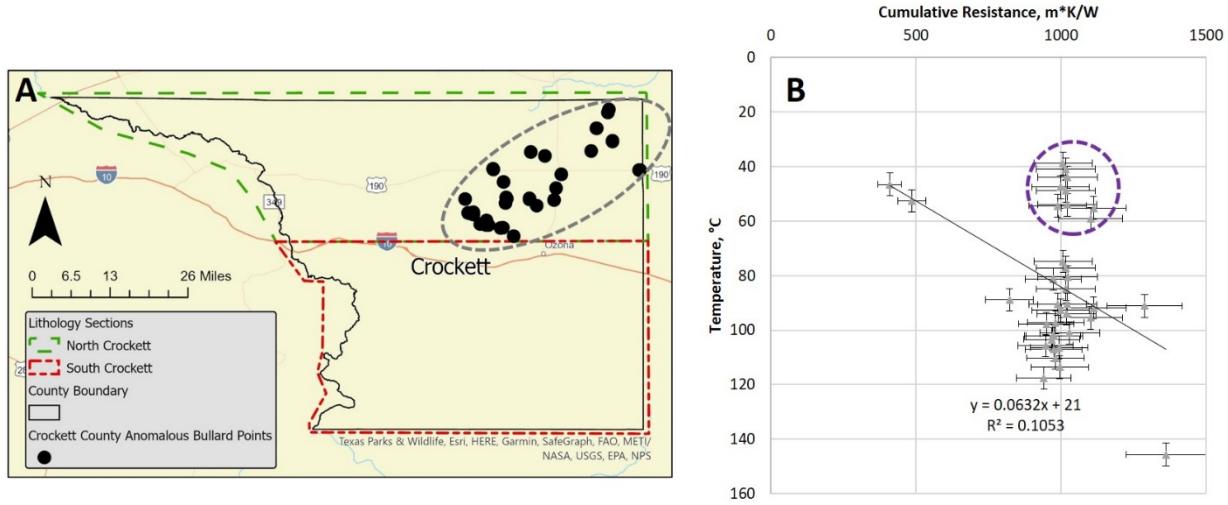

Figure 8. Outlier examination in Northeast Crockett County. (A) Location of potential outlier data (purple dashed circle) highlighted in the Bullard plot in (B). The Bullard plot examination of circled data, shows a group of lower temperature data at the same cumulative resistance. These data, after further review, contain anomalously low, non-equilibrium or gas impacted temperatures and are therefore excluded from the heat flow and temperature-at-depth mapping.

Radiogenic Heat Production Model

The radiogenic heat production (RHP) model is modified for this study to incorporate measured radiogenic heat production values for limestone, mudstone, and sandstone in Webb County (McKenna and Sharp, 1998b), and to produce realistic basement heat production (A_c) values (Table 5). Roy et al. (1968) and Lachenbruch (1968) suggested measured heat flow, in the upper few kilometers of the surface, is a combination of mantle heat flow and radiogenic heat production, which comes from sediments and the upper section of the basement. The ratio of these values in the measured heat flow is determined by the Q-A relationship (equation 1). Following the Q-A relationship, several heat flow provinces were identified (Blackwell, 1971; Blackwell et al., 1991).

$$Q = Q_m + A_s(b_s) + A_c(b_c) \quad (1)$$

Where:

Q, measured heat flow, mW/m²

Q_m, mantle heat flow, mW/m² Note: for this study it is set at 35 mW/m²

A_s, sediment radiogenic heat production, µW/m³

b_s, thickness of sediments, m

A_c, basement radiogenic heat production, µW/m³

b_c, thickness of basement radiogenic heat producing layer, m

A_c is calculated within the thermal model.

We developed different A_c calculations for each county to account for large and variable sediment thicknesses (b_c) between the three counties (Figure 9), which ultimately impacts the thickness of the basement due to isostatic equilibrium principles (Table 5). Previous studies calculated A_c following the Blackwell et al. (2006) equation, which set b_c equal to 10 km, or subtracted b_c from 13 km if it is greater than 3 km. This accurately compensated for sediment loads of around 3 to 5 km within older (Paleozoic) basins, which is appropriate for Crockett County. Webb and Jackson County, however, are Cretaceous and younger and contain maximum sediment thicknesses of approximately 10 km and 12 km, respectively. For these two counties, the Blackwell et al. (2006) thickness calculation did not produce A_c values within the known RHP range for felsic rocks (Hasterok and Webb, 2017), indicating requirement of a new model. For Webb County, b_c is calculated as 15 km minus sediment thickness to account for the average sediment thickness of 7.4 km, and in Jackson County, b_c is calculated as 20 km minus sediment thickness to account for the average sediment thickness of 10.8 km. Using these b_c values, A_c calculates to within known values for felsic rocks. Because b_c is an unknown, no measurements, tests are run to determine the model sensitivity to basement thickness calculation and discussed in the Results and Discussion section.

Similarly, A_s was previously set to 1 µW/m³ as a simplification due to lack of comprehensive RHP measurements. Here, we calculated a thickness weighted average, A_s, for each lithology section using the McKenna and Sharp (1998b) measured RHP values for the Frio mudstone and sandstone, Wilcox sandstone and mudstone, and Stuart City Limestone (Table 5). These values come from South Texas and are a good regional estimation of Texas Gulf Coast sediment thickness. The averaged A_s varied from 0.8 µW/m³ in the North Crockett lithology section to 1.4 µW/m³ in the Jackson County lithology zone. All other lithology zones are either 1 or 1.1 µW/m³. The sediment thickness, b_s, is the total sediment thickness for each individual well site, extracted from the AAPG depth to basement map (AAPG, 1978). The mantle heat production (Q_m) is a constant based on Blackwell et al. (1992).

Depth, km	Basement Radioactive Heat Production Thickness Model															
	Crockett County					Webb County					Jackson County					
1	SED	SED	SED	SED	SED	SED	SED	SED	SED	SED	SED	SED	SED	SED	SED	
2	BAS	SED	SED	SED	SED	SED	SED	SED	SED	SED	SED	SED	SED	SED	SED	
3	BAS	BAS	SED	SED	SED	SED	SED	SED	SED	SED	SED	SED	SED	SED	SED	
4	BAS	BAS	BAS	SED	SED	SED	SED	SED	SED	SED	SED	SED	SED	SED	SED	
5	BAS	BAS	BAS	BAS	SED	BAS	SED	SED	SED	SED	SED	SED	SED	SED	SED	
6	BAS	BAS	BAS	BAS	BAS	BAS	BAS	SED	SED	SED	SED	SED	SED	SED	SED	
7	BAS	BAS	BAS	BAS	BAS	BAS	BAS	BAS	SED	SED	SED	SED	SED	SED	SED	
8	BAS	BAS	BAS	BAS	BAS	BAS	BAS	BAS	BAS	SED	SED	SED	SED	SED	SED	
9	BAS	BAS	BAS	BAS	BAS	BAS	BAS	BAS	BAS	BAS	SED	SED	SED	SED	SED	
10	BAS	BAS	BAS	BAS	BAS	BAS	BAS	BAS	BAS	BAS	BAS	SED	SED	SED	SED	
11	BAS	BAS	BAS	BAS	BAS	BAS	BAS	BAS	BAS	BAS	BAS	BAS	SED	SED	SED	
12		BAS	BAS	BAS	BAS	BAS	BAS	BAS	BAS	BAS	BAS	BAS	BAS	SED	SED	
13			BAS	BAS	BAS	BAS	BAS	BAS	BAS	BAS	BAS	BAS	BAS	BAS	SED	
14						BAS	BAS	BAS	BAS	BAS	BAS	BAS	BAS	BAS	BAS	
15						BAS	BAS	BAS	BAS	BAS	BAS	BAS	BAS	BAS	BAS	
16											BAS	BAS	BAS	BAS	BAS	
17	NON RADIOACTIVE BASEMENT										BAS	BAS	BAS	BAS	BAS	
18						NON RADIOACTIVE BASEMENT					BAS	BAS	BAS	BAS	BAS	
19											BAS	BAS	BAS	BAS	BAS	
20											BAS	BAS	BAS	BAS	BAS	
21											NON RADIOACTIVE BASEMENT					
SED = overlying sedimentary rock, BAS = radioactive heat producing basement																

Figure 9. Basement radioactive heat production model thickness, b_c,. Models for each county, where SED is sedimentary rock thickness and BAS is the radioactive heat producing basement. The bottom of the temperature-at-depth modeling is 10 km, shown here with the black line. (Left) Crockett County uses the Blackwell et al. (2006) model where the b_c is a constant 10 km until sediment is greater than 3 km, and then b_c is equal to 13 km minus sediment thickness. (Center) Webb County b_c is equal to 15 km minus sediment thickness to account for the thicker sedimentary package, which has a minimum thickness of 4 km. (Right) Jackson County b_c is equal to 20 km minus sediment thickness to account for the thicker sedimentary package, which has a minimum thickness of 9 km. Using this modified thickness calculation model, basement radiogenic heat production, A_c values are within the measured values for felsic rocks (Hasterok and Webb, 2017) and are considered more representative and potential real-world geologic conditions.

Table 5. Radiogenic Heat Production Model Parameters.

Lithology Section	Q_m, mW/m²	A_s, μW/m³	b_s, m	A_c, μW/m³	b_c, m
North Crockett	35	0.8	Taken from AAPG (1978) map	Calculated	13 km – sediment thickness[+]
South Crockett	35	1.1	Taken from AAPG (1978) map	Calculated	13 km – sediment thickness[+]
Jackson	35	1.4	Taken from AAPG (1978) map	Calculated	20 km – sediment thickness[Δ]
North Webb	35	1.1	Taken from AAPG (1978) map	Calculated	15 km – sediment thickness[#]
Southwest Webb	35	1	Taken from AAPG (1978) map	Calculated	15 km – sediment thickness[#]
Southcentral Webb	35	1	Taken from AAPG (1978) map	Calculated	15 km – sediment thickness[#]
Southeast Webb	35	1.1	Taken from AAPG (1978) map	Calculated	15 km – sediment thickness[#]

Q_m set to 35 mW/m² is based on values from Blackwell et al. (1992).

[+] This is the original basement radiogenic heat production thickness model of Blackwell et al. (2006), developed for older, stable continental crust.

[Δ] This is the modified basement radiogenic heat production model. This new model is in general agreement with crustal thickness results presented by Agrawal et al. (2015) and now produces heat production values within worldwide heat production values for felsic rocks.

[#] Webb County contains a smaller and slightly older stratigraphic section of the Gulf Coast Basin. Therefore, it was assigned a combination of the Blackwell et al. (2006) model and the newly developed model for Jackson County including the recent work of Agrawal et al. (2015).

Temperature-at-depth mapping

Temperature-at-depth values are calculated after heat flow values are calculated for every data point using equation 2, the second derivative of the heat diffusion equation, following the same procedure as previous work (Blackwell et al., 2006; Stutz et al., 2015; Smith, 2016; Smith and Horowitz, 2017; Batir et al., 2019). These temperature calculations assume the study area is at steady state and heat travels through pure conduction. Calculations were made using the modified heat flow and temperature-at-depth calculation code made available through Horowitz et al. (2015). The code was modified to incorporate the different b_c thickness calculation models and other updated values such as Q_m and A_s. Inputs to the temperature model are shown in Table 2.

$$T_z = T_{surf} + \frac{(Q_s - A_s Z_s) * (Z_s)}{K_s} - \frac{A_s * (Z_s)^2}{2K_s} + \frac{Q_m * Z_{c-s}}{K_c} + \frac{A_c b_c^2 * (1 - e^{\left(-\frac{Z_{c-s}}{b_c}\right)})}{K_c} \quad (2)$$

Where:

T_z, temperature at depth (z), °C

T_{surf}, surface temperature, °C

Q_s, measured heat flow, mW/m^2

A_s, radiogenic heat production of the sedimentary section, µW/m^3

Z_s, thickness of sedimentary section, m

K_s, Thermal conductivity of sedimentary section, W/m*K

Q_m, Mantle heat flow, mW/m^2

A_c, Radiogenic heat production of the basement rocks, µW/m^3

Z_{c-s}, Thickness of basement section, m

K_c, Thermal conductivity of basement, W/m*K

b_c, Thickness of heat generation in the basement, m

Once calculated, temperature-at-depth maps are gridded using the Empirical Bayesian Kriging (EBK) interpolation algorithm within the Geostatistical Analyst toolbox in ArcGIS Pro version 2.2. The EBK interpolation method, as a kriging interpolation algorithm, is built to predict values at unmeasured locations by assuming that some of the variation within the data are natural variations associated with spatial changes in the environment. A grid spacing of 10 x 10 km was chosen following development of the interpolation semivariogram.

Results and Discussion

The collected temperature data and the determined thermal conductivity values are basis of the terrestrial heat flow calculated for 5410 well sites across Crockett, Jackson, and Webb Counties of Texas. Using these heat flow values, with incorporated detailed county level lithology and radiogenic heat production (RHP) values, each county can examine the temperatures of the subsurface through maps from 3.5 to 10 km depth. The process of calculating these temperatures includes models, which use the site-specific temperature at that depth to accurately depict the temperatures to known locations, and then incorporates surrounding well information and the other parameters (lithology, RHP) to calculate temperatures for

intermediate depths and even deeper to 10 km. The deepest BHT is 259 °C at 6.3 km depth in Webb County. In Jackson County, the BHT is 214 °C at 5.5 km depth, while in Crockett County, the deepest BHTs are on average 160 °C at 4.5 km depth. There is no direct temperature measurement, thermal conductivity, or radiogenic heat production beyond these deepest BHT values. Although there are many well sites between 3.5 km and the deepest site in each county, in general, the majority of the well data are less than 3.5 km and therefore, the temperature maps deeper than this include an additional uncertainty. Still these county heat flow and temperature maps are more realistically defined than previous maps.

Terrestrial heat flow values increased by 35, 37, and 39% for Crockett, Jackson, and Webb Counties, respectively, in comparison to past results by Blackwell et al. (2011) and Blackwell and Richards (2004) (Tables 3 and 4). The average county-wide geothermal gradient from surface to BHT (Tables 3 and 4) increased 30, 13, and 14% for Crockett, Jackson, and Webb Counties, respectively, with the additional well sites and temperature data. Using the Pitman and Rowan (2012) thermal conductivity values increased the average thermal conductivity by approximately 20% for individual wells for Jackson and Webb Counties. For Crockett County the thermal conductivity values increased by only 4% using the Anadarko Basin values (Gallardo and Blackwell, 1999; Carter et al., 1998).

The additional well data density shows significant heat flow heterogeneity, which is considered a real geological variation as opposed to increased error. All the heat flow values were calculated utilizing the same numerical model, regardless of previous heat flow determinations. Thus, the heterogeneity is the result of variation within the input data (corrected BHT and thermal conductivity) instead of variations in the heat flow calculation methodology.

There is a concern when working with temperature data with no equilibrium wells to constrain the correction. Reviewing the deepest wells in Crockett County, all located in the southwest corner of the county (Figure 10), they demonstrate a possible geological variation in heat flow and in temperature. This variation is visible even in the temperature-at-depth maps from 5 to 10 km (shown below). These wells are all gas wells between 4500 – 4650 m depth, yet vary in temperature between 130 to 176 °C. This variation, while within the standard variation of the data, requires more individual site review in order to accurately determine if the extremes represent local geology differences or drilling impacted conditions.

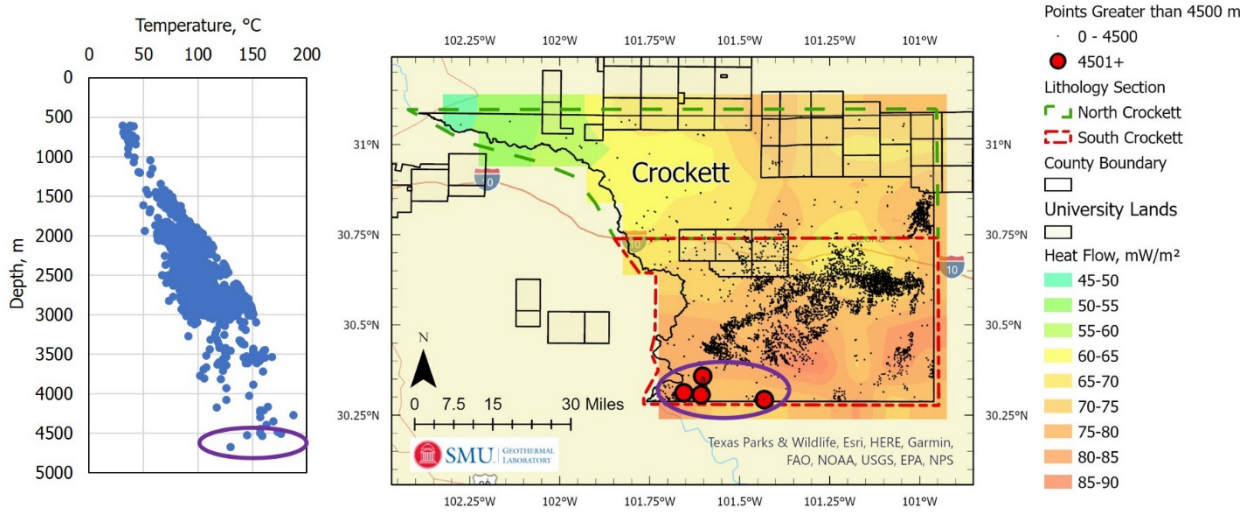

Figure 10. Crockett County temperature-depth plot with heat flow map. The blue data points are all BHT data. The deepest data points on left are < 20 km apart (right) with a temperature variation of 130 - 176 °C.

The updated sedimentary formation RHP (A_s) for this study follows McKenna and Sharp (1998b) as their data directly overlaps for Webb County. The contribution of RHP is included in the calculations for the temperature-at-depth maps. In adding this parameter to the model, the well gradients are not just extrapolated to any depth, rather modeled to incorporate lithology and heat production. The extent of model improvement with the inclusion of A_s values based on detailed lithology and measured values, is helpful for comparisons between past (Blackwell et al., 2011) and present research.

The most A_s impact is on Jackson County with the change, from 1.0 $\mu W/m^3$ to 1.4 $\mu W/m^3$. This caused the county average temperature at 10 km to decrease from 371 °C to 364 °C, respectively, or an average reduction of 7 °C per site. Jackson County has the highest A_s, and therefore the most impact occurs on the deep temperature calculations. In North Crockett the A_s value decreased from 1 $\mu W/m^3$ to a value in this study of 0.8 $\mu W/m^3$, incurring a slight increase in temperature (<5 °C) for temperatures at 10 km. All of the changes in temperature produced by the improved A_s at 10 km are approximately ± 2%, which is within the uncertainty of the correction for BHT initially applied. This is a small change, yet as projects move from research to development, the more site-specific inputs possible, the stronger the end results. See the supplementary temperature data file for the lithology thickness weighted average sedimentary RHP value.

Similarly, the amount of temperature change due to different thermal conductivity values is also examined. Jackson County contains the largest percentage of pure sandstone and shale, as well as having the largest mixed sedimentary section; therefore, Jackson County is most susceptible to temperature variation driven by thermal conductivity uncertainty. As the Pitman and Rowan (2012) values are model determined (not measurements from cores) we examined the difference between using only the reduced thermal conductivity values for all formations, instead of a mix of their values based on lithology depth and approximate *in situ* temperature. Using only the lower values decreased the weighted thermal conductivity for the lithology section by ~5% (2.16 to 2.08 $Wm^{-1}K^{-1}$, respectively) and this impacted the 10 km temperatures in Jackson County from an average of 364 to 348 °C, respectively. This average temperature variation of 12 °C, is less than 10% of the mapped values and is within the uncertainty of BHT corrections and heat flow measurement uncertainty. Combining the decrease of the A_s and the lower thermal conductivity values, the temperature change on average is -23 °C or (from 371 to 348 °C), which is still less than 10% of the mapped temperature value.

The final source for error in the temperature-at-depth models are the model derived A_c, (basement RHP). The impact is small from the modifications in sediment thickness to lower the depths from 13 km to 15 km in Webb County and to 20 km in Jackson County, as the difference in temperatures at 10 km are again within BHT correction temperature error. The basement has a constant heat contribution following the Q-A relationship, meaning that any temperature calculation above the basement receives contribution from the entire basement RHP. The distribution of this heat contribution is what we vary within the model by using individualized basement RHP layer thickness models for each county, modified from the original thickness calculation of Blackwell et al. (2006). This variation in heat distribution within the basement will impact temperature calculations that reach into the basement. Crockett County uses the Blackwell et al. (2006) model because it is an older, shallower basin and a modification was not necessary. Jackson County and Webb County were modified to account for the large, young sedimentary packages in these parts of the Gulf Coast Basin. Temperatures at 10 km depth were compared to see how Jackson and Webb County and their respective new thickness calculations impacted temperature uncertainty. The 10 km depth was chosen because it is the deepest temperature calculation and would be most impacted by this thickness model change. The average temperature for Webb County at 10 km slightly increases from 375 °C for the original model to an average of 377 °C. Similarly, in Jackson County, the average temperature

at 10 km increases from 364 °C in the original model to a 371 °C in the new model. Based on these results, the basement RHP thickness impacts the temperature at 10 km by less than 2%.

In reviewing all the possible input uncertainty results discussed above, each one shows that the uncertainty of the mapped temperatures at 10 km is low for any given parameter. The result of their combined uncertainty less than 15%, which is less than the uncertainty associated with BHT derived heat flow of 25%. As the temperature is calculated beyond 10 km depth and into the basement RHP layer, however, the RHP distribution becomes a more significant component of the temperature calculation. Any temperature calculations beyond 10 km require measured values of basement RHP to confirm or modify the basement RHP model.

Heat Flow Maps

The 2020 mapping of heat flow for Crockett, Jackson, and Webb Counties (Figures 11, 12, and 13) increases in amount for all three counties with the addition of new larger data set. This increase is based on the Blackwell et al. (2011) SMU Geothermal Laboratory Heat Flow Map of the Conterminous United States (Blackwell et al., 2011b). Since the work was completed at a state to regional level, the maps for each county are extracted from the U.S. map. General heat flow trends between the SMU 2011 and 2020 maps show similarities for all three counties, although the changes in spatial resolution and higher values in the new heat flow maps are visible. Below are discussions comparing these maps on a county basis.

Crockett County

Crockett County heat flow maps (Figure 11) show a similar trend of low heat flow in the upper northwest corner of the county and increases towards the east and south. The major trend deviation occurs in the southeast corner of the county where the 2011 map decreases in heat flow again, the 2020 map increases slightly. Geothermal gradient increased by 30% for Crockett County with the addition of new data and the county average heat flow is 20 mW/m² higher for the new versus old dataset. This change in heat flow pattern and higher value is attributed to the increased data, which shows that the thermal regime in fact does increases to the southeast.

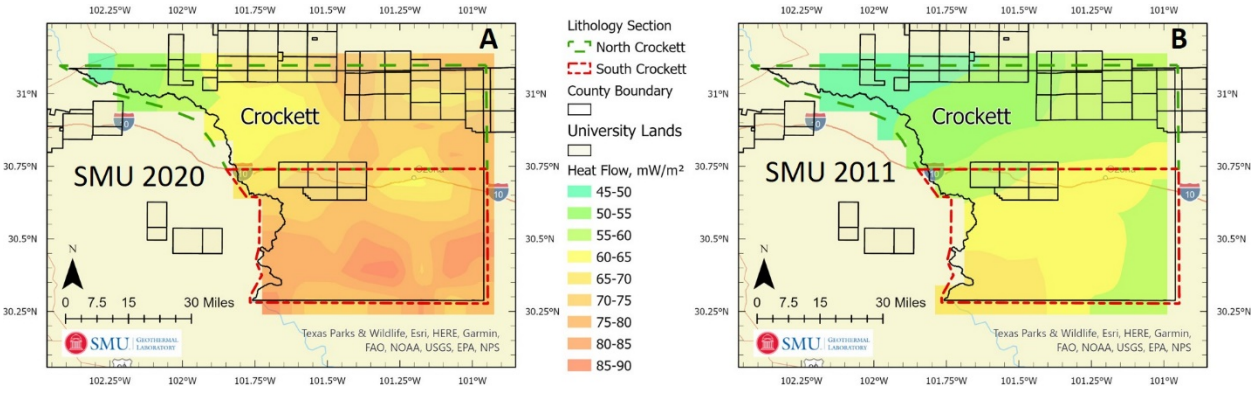

Figure 11. Heat flow comparison for Crockett County. (A) New map produced as part of the SMU 2020 assessment. (B) The SMU 2011 subset of U.S. heat flow map.

Jackson County

Jackson County shows a similar trend between the 2020 and the 2011 heat flow maps (Figure 12), going from higher heat flow in the northwest portion of the county and decreasing slightly to the southeast. Spatial resolution increased between the 2020 and the 2011 datasets, which produced a different gridding pattern, but the general trends are consistent. In Jackson County, the county average geothermal gradient increased by 13% and the well site average modeled thermal conductivity increased by 20%, which produced a county average heat flow 22 mW/m² higher in the new dataset. The increased gradient shows there is support for the increased values, although the increase in heat flow is more directly tied to the new, higher thermal conductivity model.

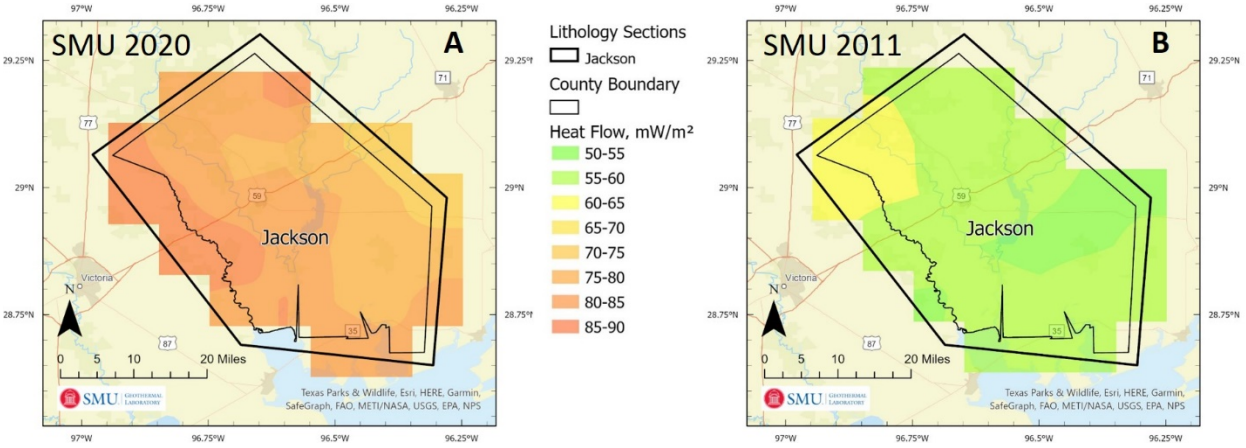

Figure 12. Heat flow comparison for Jackson County. (A) New map produced as part of the SMU 2020 assessment. (B) The SMU 2011 subset of U.S. heat flow map.

Webb County

The Webb County heat flow maps (Figure 13) show a general increase in heat flow moving from the northwest portion of the county to the southeast portion, although there are distinct changes between the two maps. In the 2011 heat flow map, there is a trend of lower heat flow in the central portion of the county and a general increase as you move away from that area. This low heat flow trend is not visible in the 2020 heat flow map, but instead includes a higher heat flow locality. This area of higher heat contains more data (see Figure 3) than 2011 project. As often is the case, this region could benefit from additional data collection to confirm this change in heat flow signature. The largest high heat flow region for both the 2011 and the 2020 heat flow maps is the south and southeast portion of the county. Geothermal gradients increased by 14% from the 2011 to the 2020 Webb County dataset, and well site average thermal conductivity increased by 20%, which produces a county average heat flow increase of 26 mW/m². Similar to Jackson County, the increase in geothermal gradient supports the increase in heat flow through direct measurement, although the heat flow increase is again more directly tied to the new thermal conductivity calculation model, which is producing higher well site average thermal conductivities.

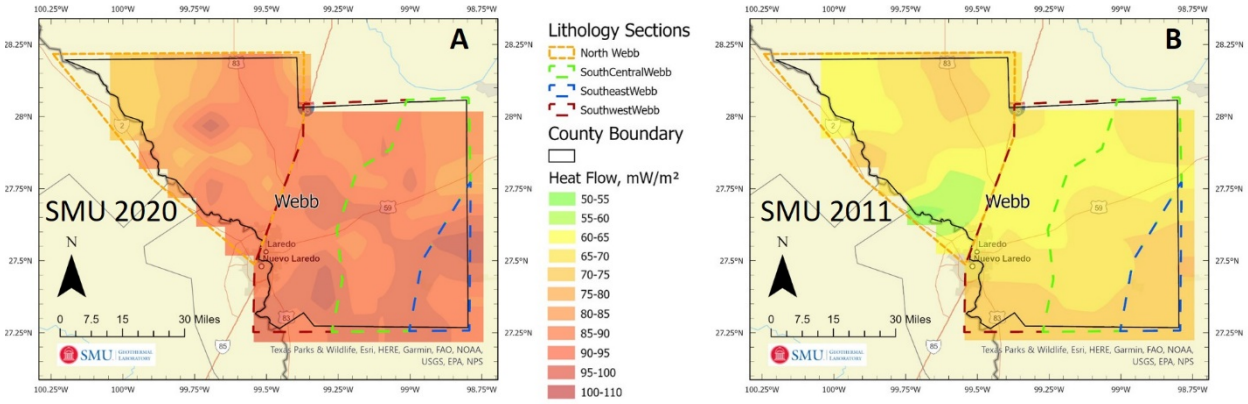

Figure 13. Heat flow comparison for Webb County. (A) New map produced as part of the SMU 2020 assessment. (B) The SMU 2011 subset of U.S. heat flow map.

Temperature Maps 3 km to 10 km

Temperature was calculated from surface to 10 km. Temperature-at-depth maps are presented here for depth slices 3.5, 5.0, 6.5, and 10 km. The 3.5 km depth slice contains the most direct measurement correlation (see Figure 3 for temperature – depth scatter plots for each county and well locations). The 5.0 km depth slice is the limit of temperature measurement, and the 6.5 and 10 km depth slices are calculated temperature models based on the input data. That is, the deepest temperature measurement is 6.3 km deep, and therefore, there are no direct temperature measurements below 6.5 km. The 6.5 km depth slice is considered the current technical depth limit for geothermal energy production. The 10 km depth slice is presented as a future depth goal for geothermal energy production with increased technology development and innovation.

The Harrison correction increased the raw average BHT by 17% for Crockett County, 14.6% for Jackson County, and 13.3 % for Webb County. The temperature-depth plots for each county show generally consistent geothermal gradients for each county (Figure 3). Measured temperatures of 150 °C in all three counties between 3.0 and 3.5 km depth show that drilling is already into formations with potential for geothermal electrical production based on temperature.

The heat flow calculation and temperature models are fitted to the corrected BHT measurement so that BHT is exactly estimated at the BHT measurement depth. In areas with multiple measurements within the 10 x 10 km grid cell, the values are averaged. Given that there are numerous wells in the 3 to 4 km depth range, we estimate the temperature-at-depth maps at 3.5 km have an uncertainty less than the BHT derived heat flow uncertainty of ±25%. The 3.5 km depth contains BHT measurements to directly support the mapped temperature, although there is not complete data coverage. Temperature maps at 5 km and beyond have an uncertainty of ±25%, equivalent to the estimated error associated with BHT derived heat flow (Richards et al., 2012). Deeper equilibrium temperature logs and local thermal conductivity measurements are necessary to reduce the uncertainty in the deeper modeled temperature values.

Crockett County

Crockett County temperature-at-depth maps are presented for the 3.5, 5.0, 6.5, and 10 km depth slices (Figures 14, 15, 16, and 17, respectively). The highest temperatures at the respective depths are in the southern and eastern portions of the county. Temperatures are not above 150 °C on University Lands boundaries until 5 km depth, although there are areas at 125 – 150 °C at 3.5 km depth, which may be prospective for geothermal electricity generation utilizing new low temperature technologies. The

southern region of the county, as part of the Val Verde Basin, may be prospective for geothermal electricity production, which could be immediately utilized in ongoing oil and gas exploration and production.

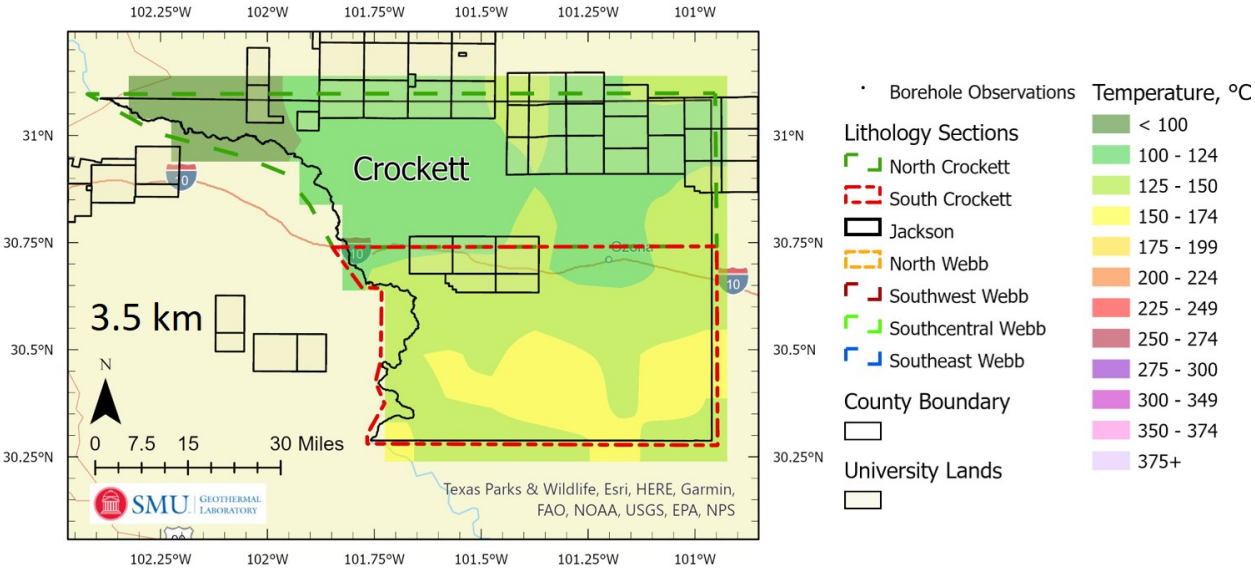

Figure 14. Crockett County temperature at 3.5 km depth. The temperature shows a general increasing from the north and west to the south and east.

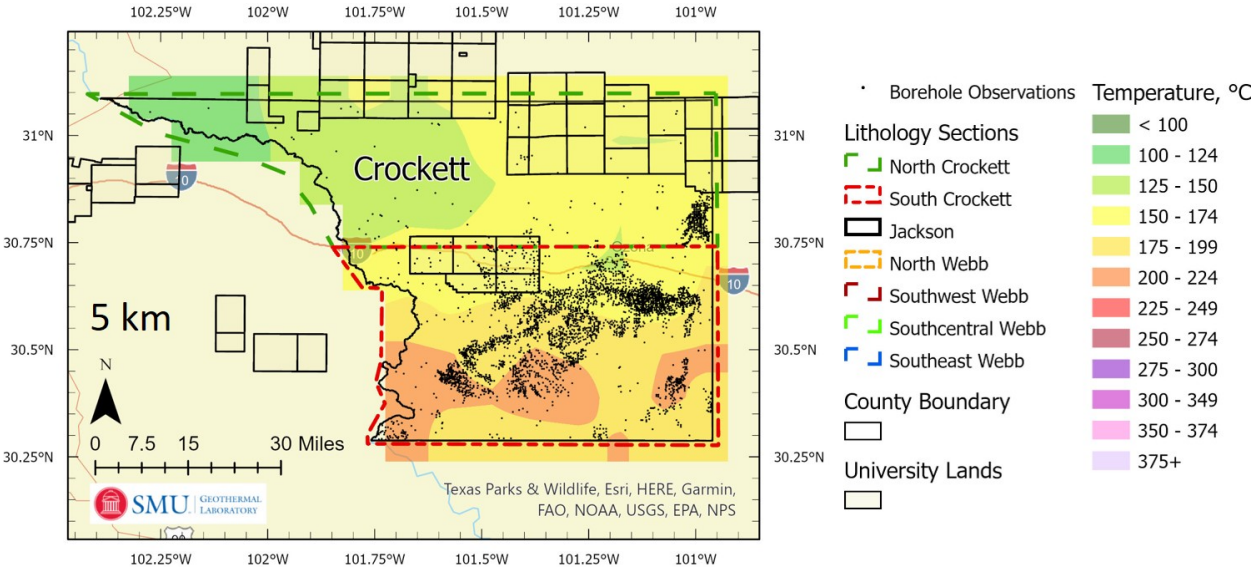

Figure 15. Crockett County temperature at 5.0 km depth. A similar trend of warmer temperatures going from the northwest to south and east is visible. Surface well locations are displayed as small black dots for reference, yet not drilled to this depth. Several large temperature trends are supported by large groups of data. The majority of Crockett County is over 150 °C at this depth.

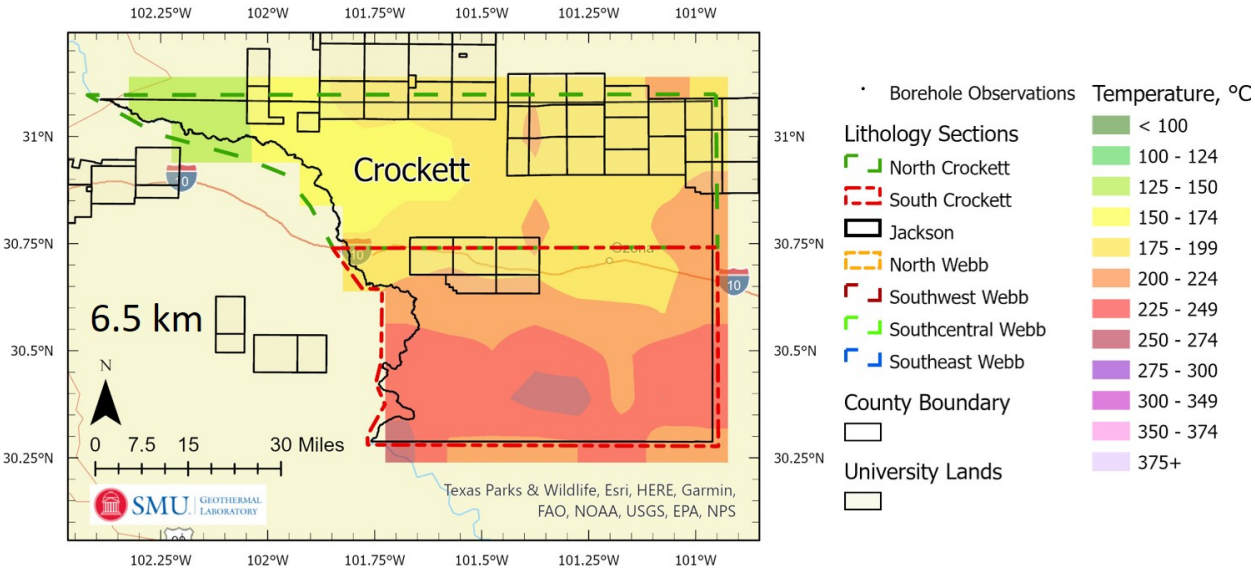

Figure 16. Crockett County temperature at 6.5 km depth. A similar trend is seen here with temperature increasing at this depth when moving from the northwest to the east and south. The hottest temperatures at this depth are between 225 and 250 °C.

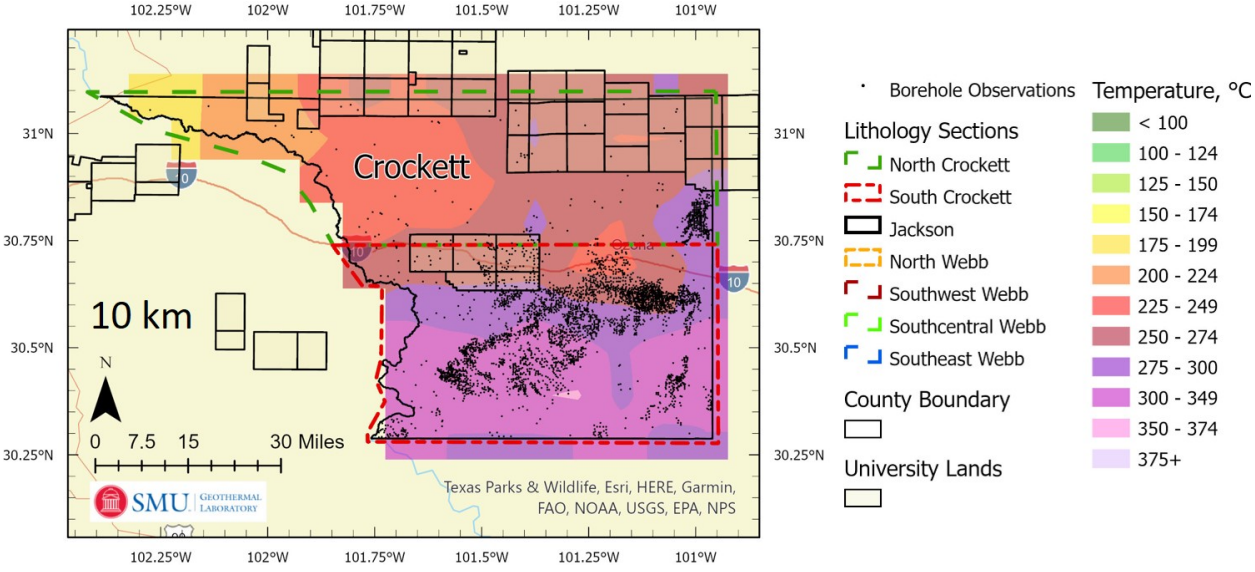

Figure 17. Crockett County temperature at 10 km, with surface well locations displayed as small black dots. While data sites are displayed on this map, there are not direct temperature measurements at this depth.

Jackson County

Jackson County temperatures at 3.5, 5.0, 6.5, and 10 km are presented in (Figures 18, 19, 20, and 21, respectively). Modeled temperatures are warmer along the western and northern boundary of the county and generally lower to the east. This trend becomes more pronounced with increasing depth, although temperatures at 6.5 and 10 km are strictly modeled temperatures and therefore include more uncertainty.

The higher temperatures along the western mapped boundary suggests there is geothermal electricity potential that could be utilized by Victoria or for industrial purposes near Lavaca Bay.

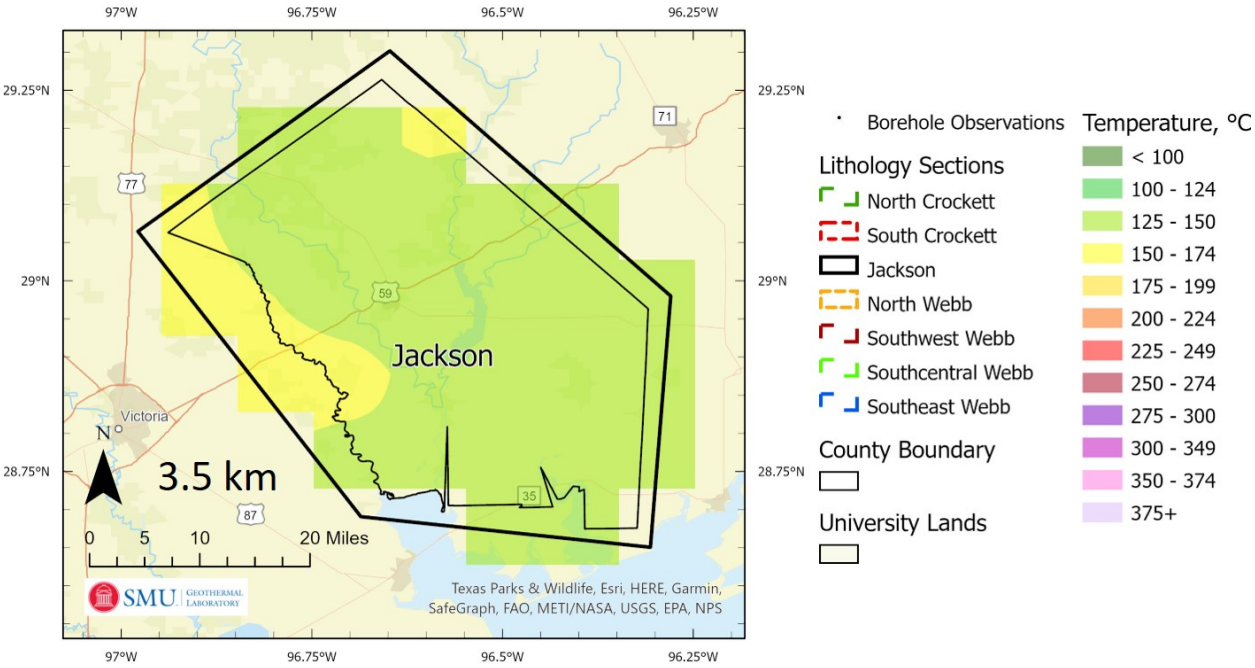

Figure 18. Temperature at 3.5 km depth in Jackson County. Higher temperatures are mapped along the western boundary and near the northern corner of the county.

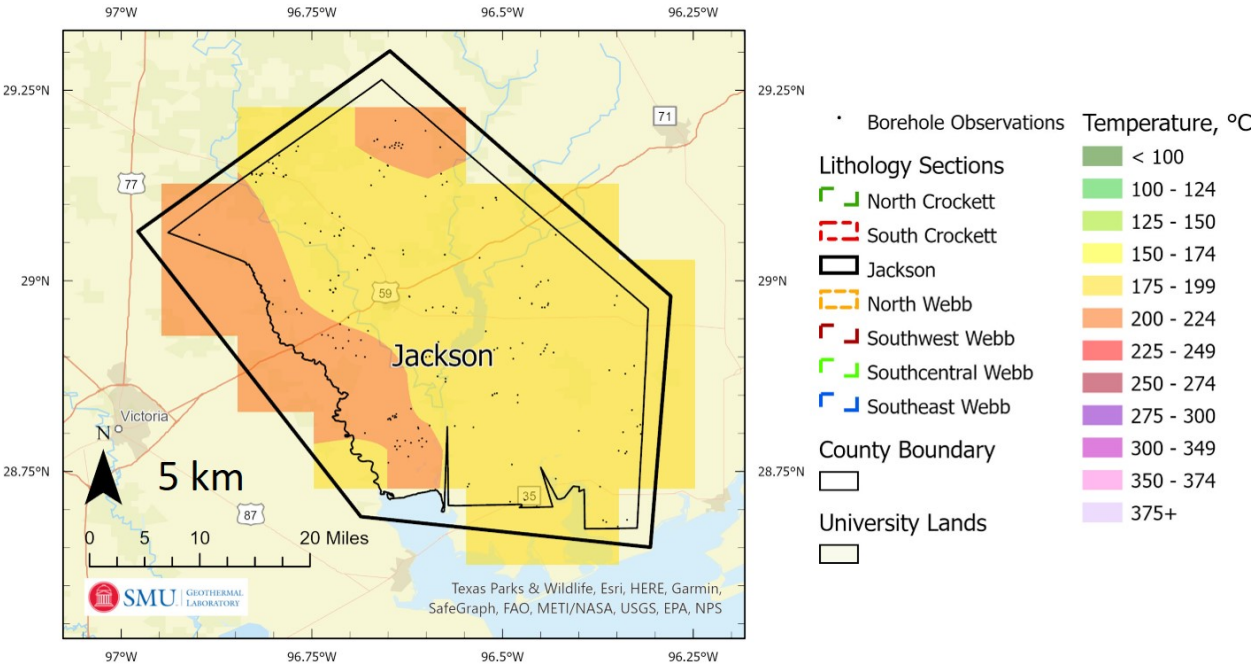

Figure 19. Temperature at 5.0 km depth in Jackson County, with data sites shown as small black dots for reference, yet not to indicate drilled to this depth. This is the deepest temperature map with near direct temperature measurements to support the temperature gridding. At this depth the whole county is above 150 °C

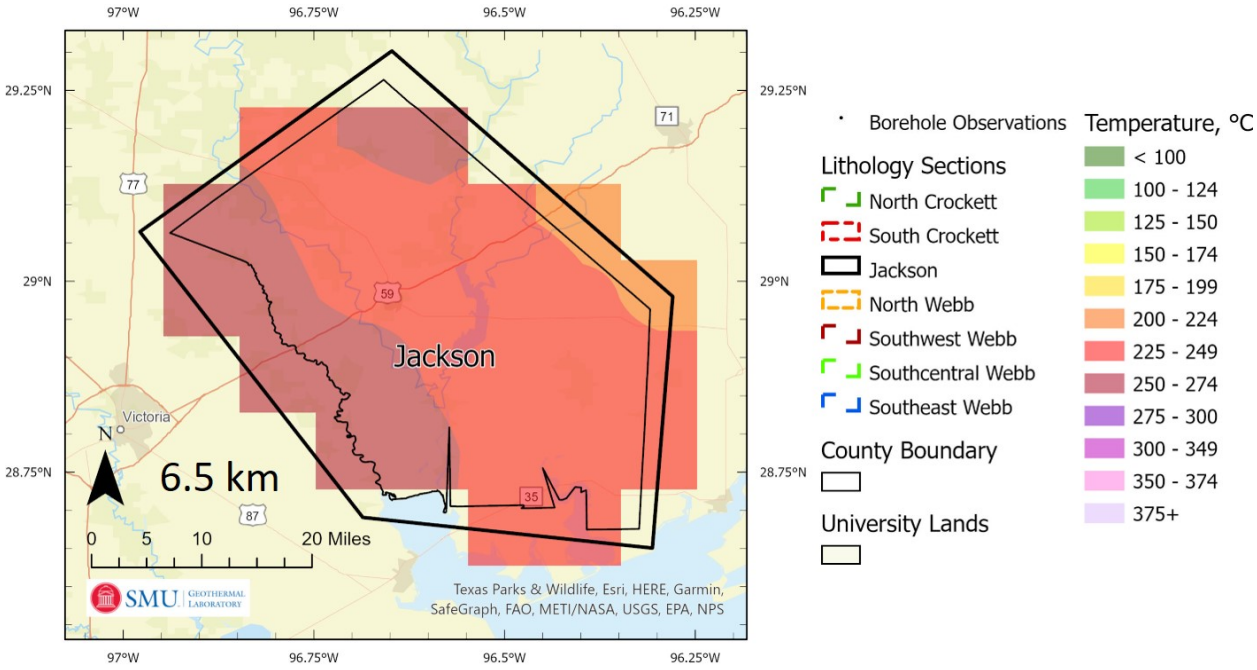

Figure 20. Modeled temperature at 6.5 km depth in Jackson County. There is a similar trend of high temperature along the western boundary in the the northern tip of the county, although there are not direct measurements at this depth.

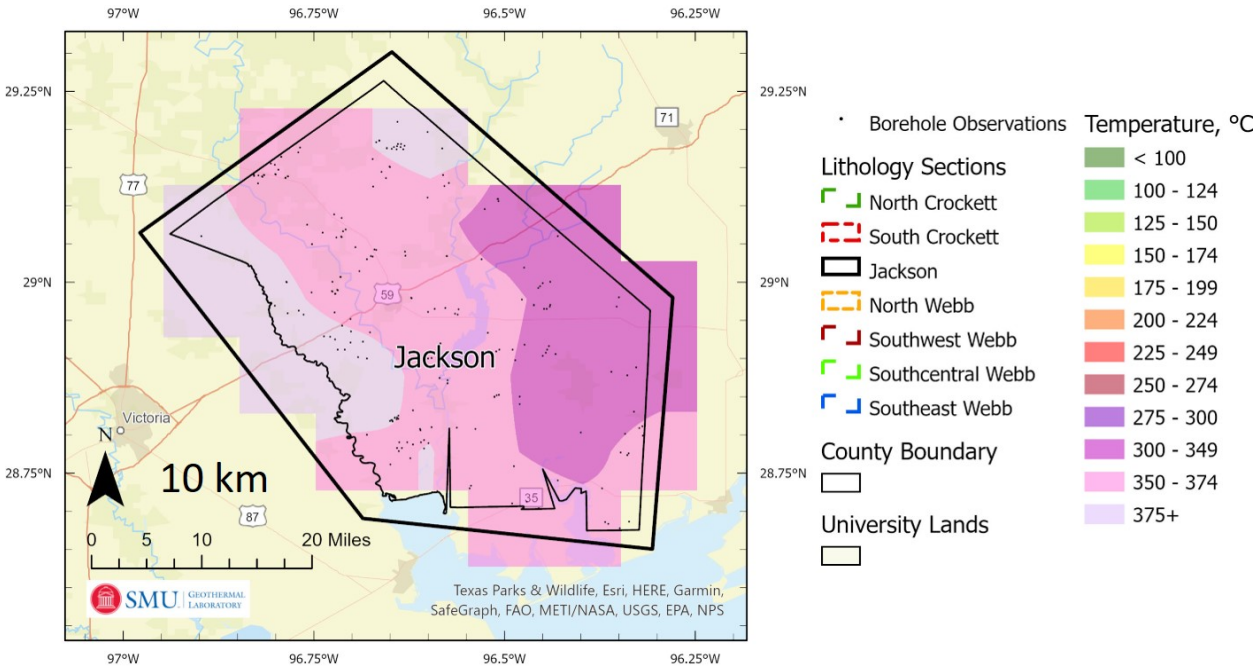

Figure 21. Modeled temperature at 10 km depth in Jackson County. While the entire county contains high temperatures, there are no direct temperature measurements at this depth and uncertainty is ±25%, which could be as high as ±100 °C. The temperatures for 10 km range from 300 to 375+ °C.

Webb County

Temperature at depth 3.5, 5.0, 6.5, and 10 km are presented for Webb County (Figures 22, 23, 24, and 25, respectively). Webb County shows a general trend of warmer temperatures moving from the northwest to the southeast. The city of Laredo has estimated temperatures at 150 – 174 °C at 3.5 km, which is prospective for geothermal electricity production using enhanced geothermal systems (EGS) technology. There are large numbers of data in the 3 to 4 km depth range that support these temperature estimates (see Figure 3). These temperature trends are modeled to continue in a similar pattern to 10 km depth, although there is only 1 data point deeper than 5 km, which is 258 °C at 6.28 km.

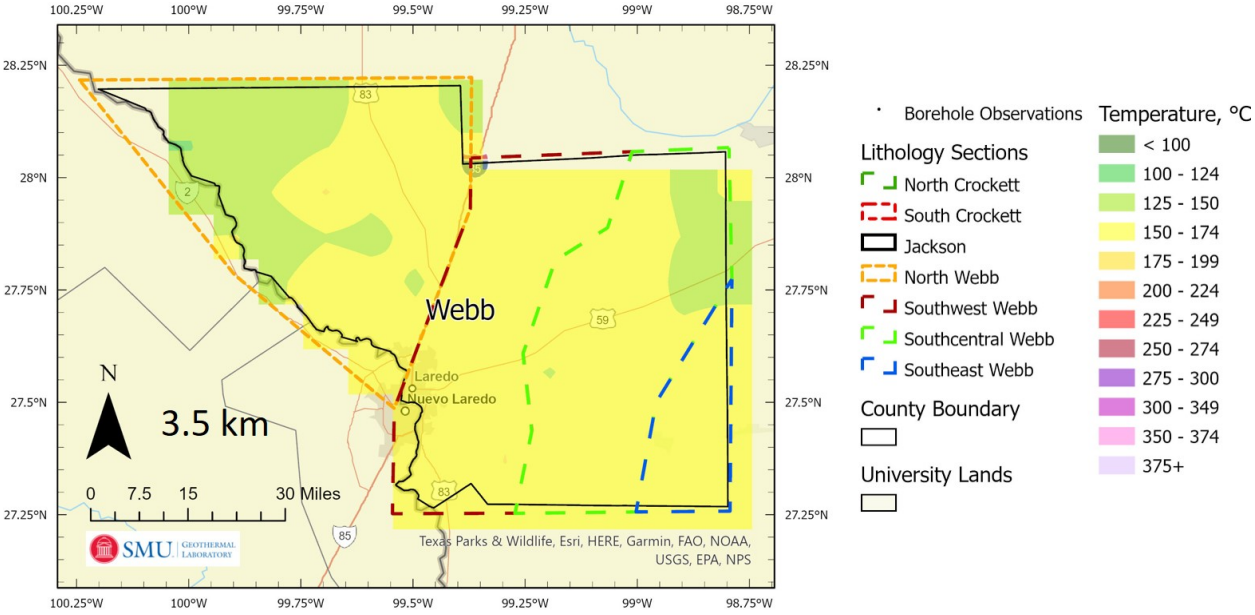

Figure 22. Temperature at 3.5 km depth in Webb County. The majority of the county is within the 150 - 174 °C temperature range. The only areas outside this temperature range are the northwestern and eastern corners of the county.

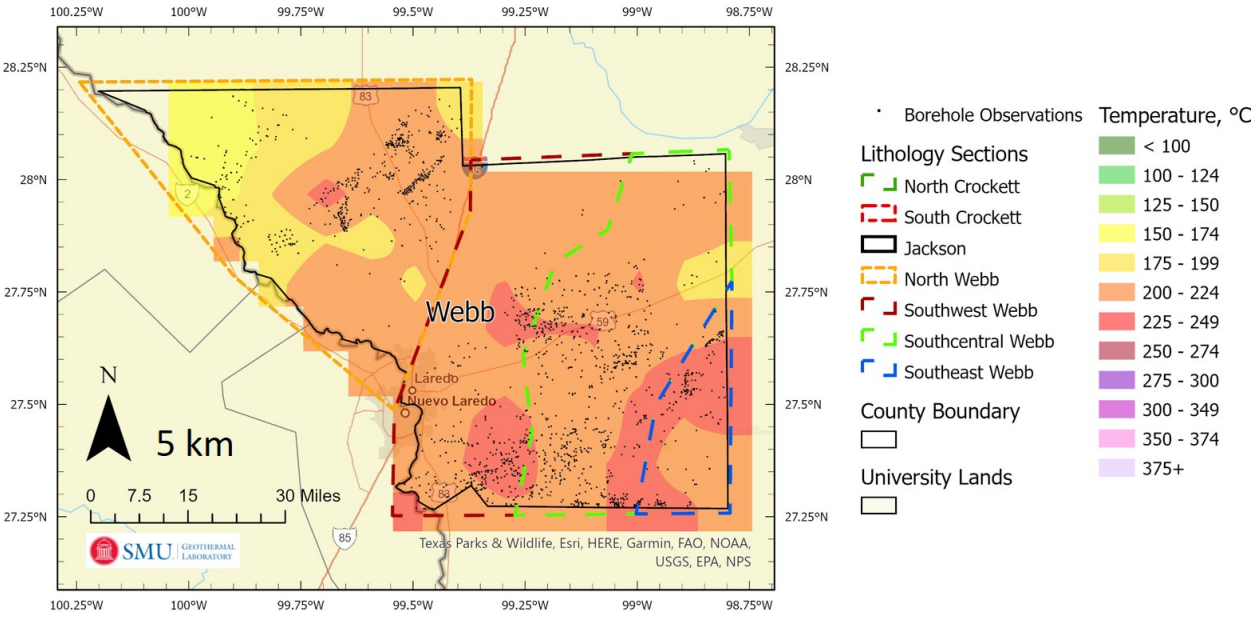

Figure 23. Temperature at 5.0 km depth in Webb County. Data point locations displayed as black dots, yet they do not to indicate drilling to this depth. While all the data are shown, there are only 2 data points at or below 5 km, both of which are above 200 °C.

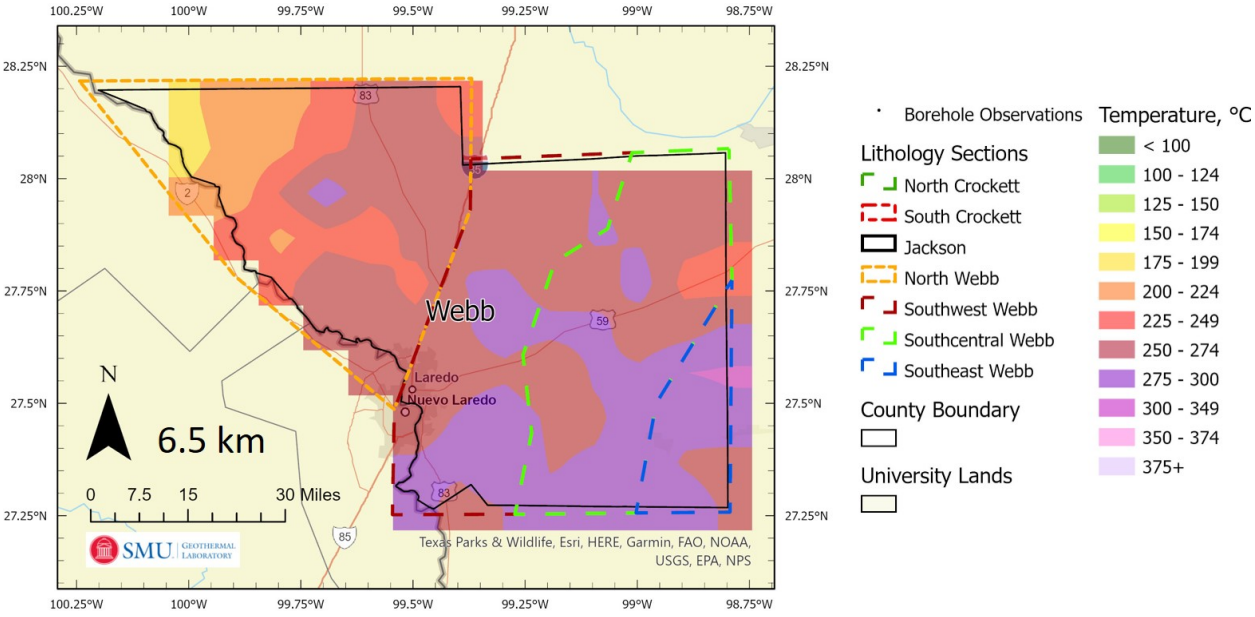

Figure 24. Modeled temperature at 6.5 km in Webb County. The areas around Laredo show prospective high temperature regions, which may be an ideal target for future technology testing. The southeast quadrant is approximately 275 °C.

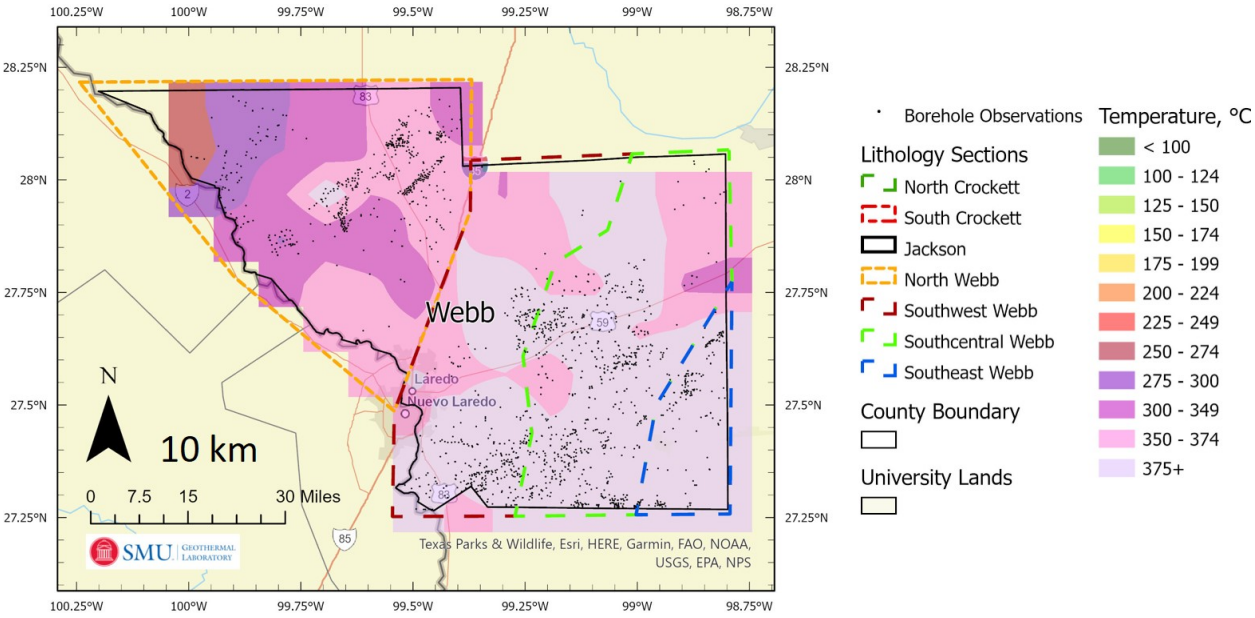

Figure 25. Modeled temperature at 10 km in Webb County. Surface well locations displayed as black dots. The highest modeled temperatures continue to be in the southeastern portion of the county, which suggests there may be additional geotheramal resources continuing to the south and east of Webb County.

Comparison to Previous Work by SMU in 2011

Temperature-at-depth maps at 3.5 km and at 10 km were compared between this work and the 2011 SMU maps (Blackwell et al., 2011a). In Crockett and Webb Counties, there are similar trends on the location of warmer and cooler temperatures at the respective depths, although there are also differences. Jackson County has more apparent differences discussed in detail below. Beyond the general trends, the new maps estimate higher temperatures and show more variability, which are both results of the increased size of the dataset and the increased complexity of the temperature-at-depth models.

Crockett County

The new temperature estimates for Crockett County suggest temperatures are warmer than previously thought. A significant difference is the hotter estimated temperatures in the southeastern corner of the county (Figures 26 and 27). This increase in temperature estimates coincides with a large increase in data in the southeast corner, suggesting that the higher temperature trend is likely to occur along the entire southern portion of the county.

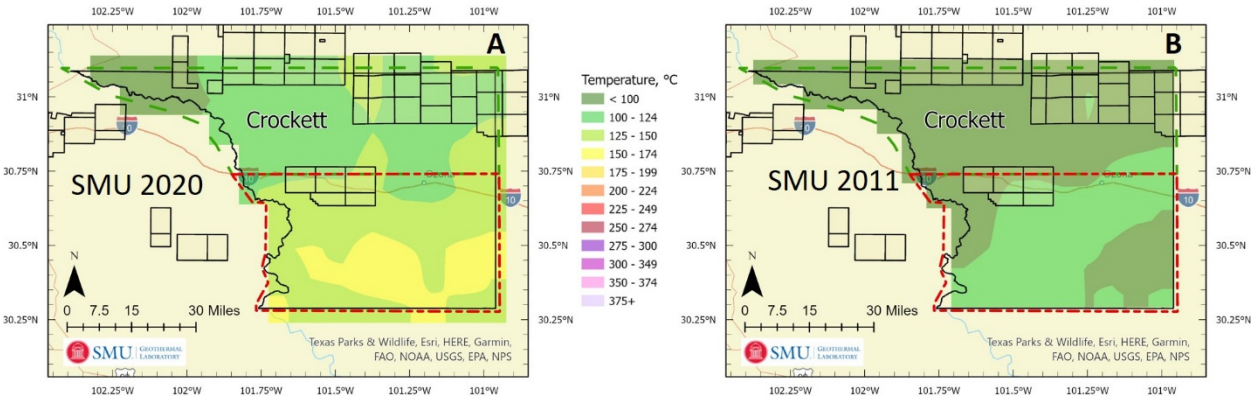

Figure 26. Temperature comparison at 3.5 km for Crockett County. (A) The 2020 temperature map. (B) The 2011 temperature map. The 2020 map shows band of 150 – 174 °C temperature along the southern county boundary, whereas the 2011 map is cooler and with less definition of a warmer trend.

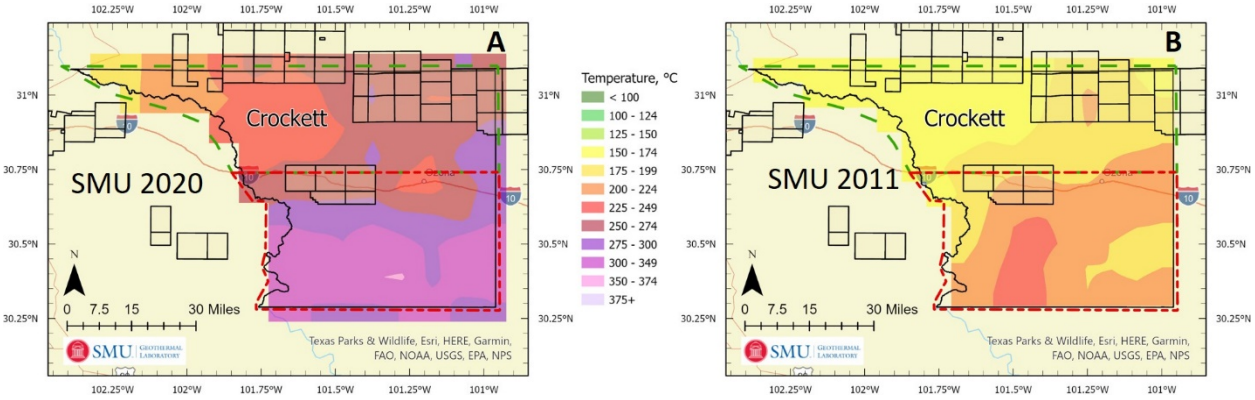

Figure 27. Temperature comparison at 10 km for Crockett County. (A) The 2020 temperature map. (B) The 2011 temperature map. Similar trends are shown here at the 10 km depth, although the temperature difference between the maps increases.

Jackson County

Jackson County shows the most difference between the 2020 SMU temperature maps and the 2011 SMU temperature maps (Figures 28 and 29) (Blackwell et al., 2011a). The 2011 maps show a decreasing temperature from the north to the south, which follows sediment thickness based on the previous thermal conductivity model (Blackwell and Richards, 2004). The new 2020 maps have temperature decreasing from west to east with some minor elongation of isotherms in the southwest to northeast direction. This difference in maps is a function of both the increased data density as well as the updated thermal conductivity model. The increased data show that geothermal gradient does not follow sediment thickness, and the calculated well site thermal conductivity, as a function of the well depth, loosely follows the total sediment thickness, but not as a linear relationship. Newly calculated well site calculated thermal conductivity is lowest in north of the county at around 2.25 $Wm^{-1}K^{-1}$, highest in the middle of the county at around 2.45 $Wm^{-1}K^{-1}$, and then drops again in the south of the county at around 2.35 $Wm^{-1}K^{-1}$. Given these trends in geothermal gradient and thermal conductivity, the 2020 heat flow and temperature-at-depth models are less correlated to the sediment thickness.

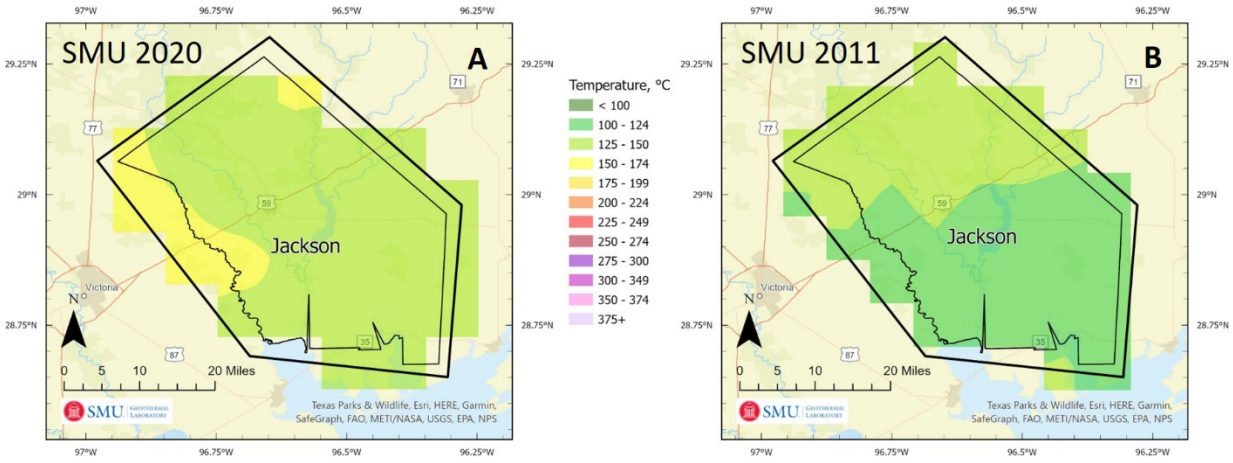

Figure 28. Temperature at 3.5 km depth comparison in Jackson County. (A) The 2020 temperautre map. (B) The 2011 temperature map. Temperatures in the 2011 map show a clear north - south decreasing temperature trending, which mirrors sediment thickness. This is in contrast to the 2020 map, which does not readily show a the similar north – south temperature trend.

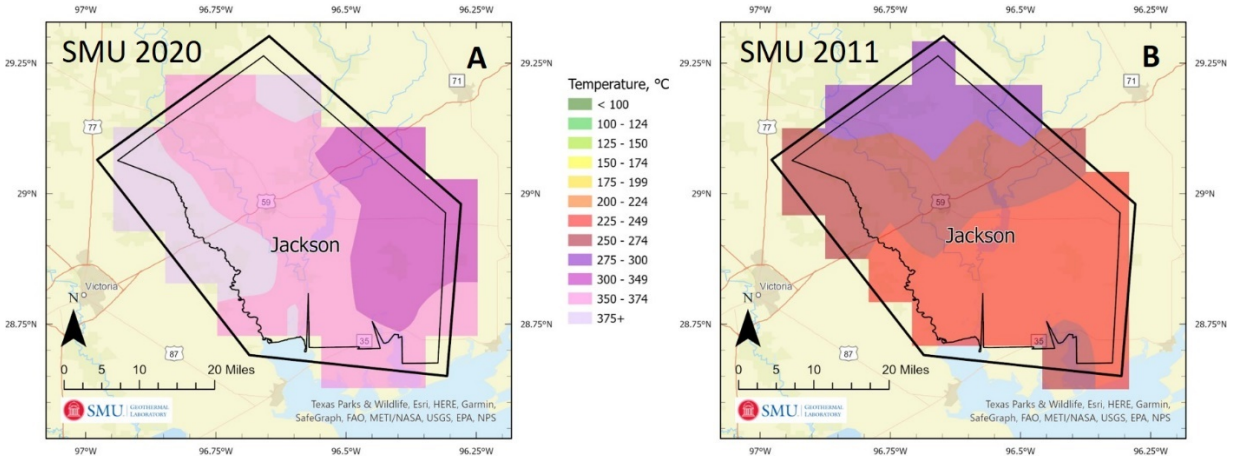

Figure 29. Temperature at 10 km depth comparison in Jackson County. (A) The 2020 temperature map. (B) The 2011 temperature map. The north – south trend is still clear in the 2011 temperature map and is not readily evident in the 2020 temperature map. There is some southwest – northeast elongation of the temperature contours visible in the 2020 temperature map, which shows suggests there is a correlation to the sediment thickness which needs to be more studied for temperature estimates at this depth.

Webb County

Temperature comparisons for Webb County at 3.5 and 10 km depth between the 2020 SMU temperature maps and the 2011 SMU temperature maps (Blackwell et al., 2011a) show similar temperature trends with increased variability and hotter modeled temperatures in the 2020 maps (Figures 30 and 31). There is an estimated 25 – 50 °C increase in temperature at 3.5 km depth, whereas there is an estimated 75 – 125 °C increase at 10 km depth going from the 2011 to the 2020 temperature maps. The 3.5 km depth temperature increase is probable and is supported by the corrected BHT measurements; the 10 km depth

temperature increase, however, needs to be confirmed with additional data collection since there is no direct measurements of temperature at 10 km depth.

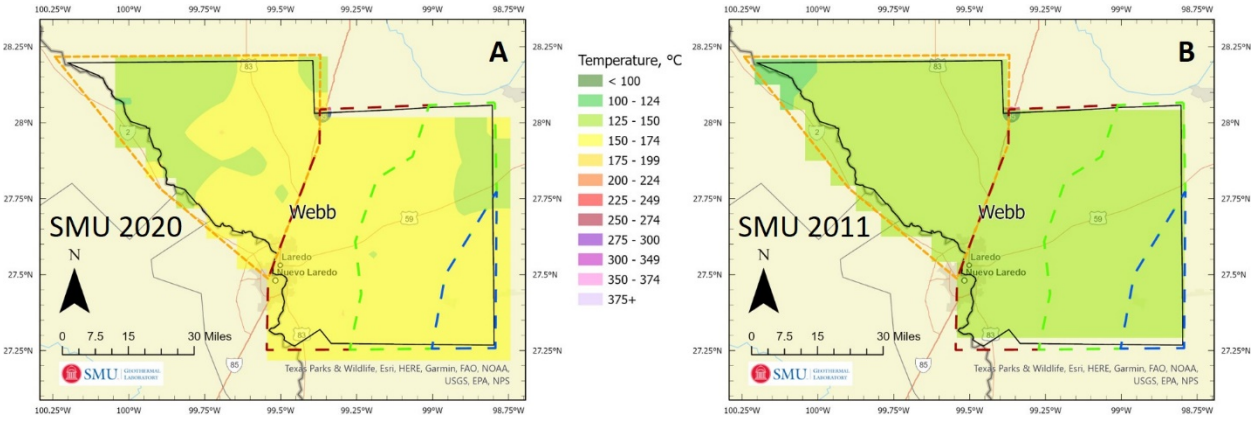

Figure 30. Temperature comparison at 3.5 km depth in Webb County. (A) The 2020 temperature map. (B) The 2011 temperature map. The majority of the county contains a uniform temperature and the 2020 projects the temperature to be 25 - 50 °C higher.

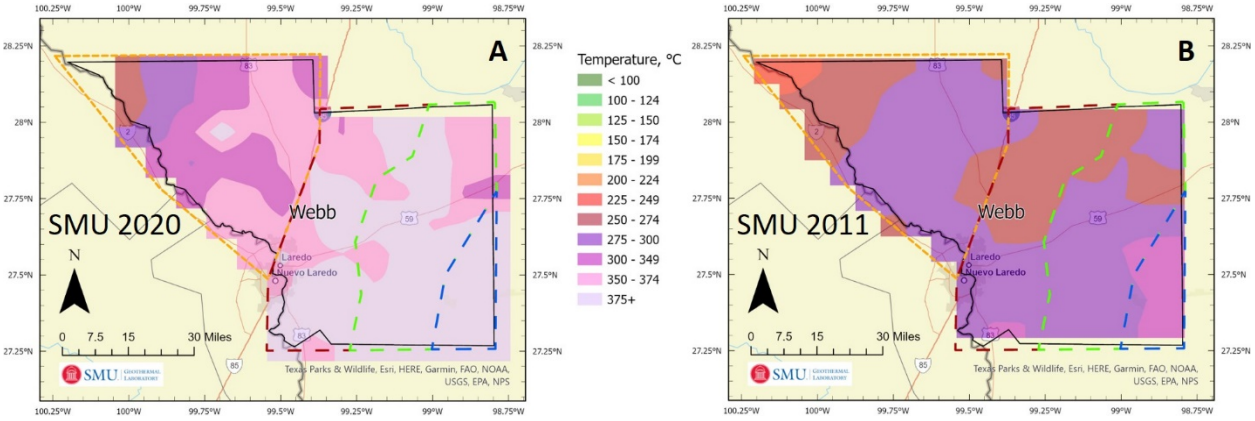

Figure 31. Temperature comparison at 10 km depth in Webb County. (A) The 2020 temperature map. (B) The 2011 temperature map. Both maps show a general increasing temperature from the northwest to the south and east, although higher temperatures are more pervasive in the 2020 map. Temperatures are expected to be higher at 10 km depth than the 2011 map suggests based on these new results, although more data need to be collected to more accurately predict temperatures at 10 km depth.

Comparison to 2012 BEG Temperature Estimates

Zafar and Cutright (2014) estimated the depth to the 232 °C isotherm using gradient from corrected BHT values. Geothermal gradient derived temperature extrapolation does not account for radiogenic heat production and may overestimate temperature at deeper depths since it does not remove the radiogenic heat component. Here, we compare the estimated depth to 232 °C using the 2020 temperature model to the Zafar and Cutright (2014) depth map. Zafar and Cutright (2014) estimate the depth to 232 °C for Crockett County to be 4.5 to 7.5+ km, with the shallow 4.5 km depths in the southern part of the county. Our 2020 temperature model shows depths to the 232 °C isotherm vary from 4.3 km to greater than 10

km, with an average value of 7.1 km after removing the data points that did not reach the projected temperature. The shallowest section in our results is also located in the southern region of Crockett County. For Jackson County, Zafar and Cutright (2014) have a nearly uniform map showing the depth to 232 °C to be 5.25 to 6 km. Our results show the depth to 232 °C varies from 4.9 to 9 km depth, with an average value of 6.2 km. For Webb County, Zafar and Cutright (2014) show the depth to 232 °C varies from 4.5 to 6 km, with the shallowest section in the southeast region of the county. Our results show the depth to 232 °C varies from 4.3 to 9.4 km with an average value of 5.5 km. Similarly, the shallowest section is the southeastern region of the county.

The general trends shown in Zafar and Cutright (2014) agree with the results presented here, although these new results contain more variability and resolution because of the incorporation of thermal conductivity and radiogenic heat production. The Zafar and Cutright (2014) results are useful for large scale reconnaissance studies examining regional geologic trends, whereas our methodology and results are better suited for more focused, early stage exploration.

Conclusions

Work performed on this project calculated new heat flow values for 5,824 points (5410 surface locations) in Crockett, Jackson, and Webb Counties. This effort for heat flow is an increase of 10x the previously used data (532 points), for these three counties. In addition, we built detailed lithology sections based on the county geology, and new thermal conductivity models, basing them on related published models, core measurements, and mineral-matrix derived thermal conductivity values. These combine to expand the density and heterogeneity of the county temperature-at-depth maps from the surface down.

The new results show heat flow are higher than previously calculated published results, generally by 30 to 40%. This is reflective of the large dataset containing a 13 – 30% higher geothermal gradient, and a 4 – 20% increase in thermal conductivity estimates. The error associated with these increases builds on the starting error with each parameter. For the geothermal gradient there is up to 10% error for the BHT measurement, which a correction is applied to reduce potential error. For the thermal conductivity the error is typically stated as 10% based on measured values, yet these results use no direct measurements for these counties, instead use a combination of published values still estimated at ~10% error.

Corrected temperatures are calculated and then mapped for specific depth of 3.5, 5.0, 6.5, and 10 km. Temperature-at-depth modeling incorporated the detailed lithology models, along with improved inclusion of sedimentary radiogenic heat production from measured values, and updated basement radiogenic heat production models to account for the thick sedimentary package of the Texas Gulf Coast. Temperatures are on average, 25 – 50 °C warmer at 3.5 km and 50 – 100 °C warmer at 6.5 km. Both of these measurements are on the order of a 50% increase in temperature. Data points greater than 3 km depth are 139 in Crockett County, 72 in Jackson County, and 786 in Webb County, whereas there is only 1 data point, at 6.28 km, in Webb County, 2 data points greater than 5 km in Jackson County, and 4 data points greater than 4.5 km in Crockett County. The 3.5 km temperature-at-depth calculation is directly supported by measured BHT, therefore temperatures below 3.5 km have limited direct support from measured values. Temperature maps are presented for 6.5 and 10 km; these deeper depth maps are considered best knowledge and not definitive of actual values at these depths. They are to be used as a tool for future research and not used for site-specific evaluations.

The temperature-at-depth model also includes calculations focused on a new basement radiogenic heat production model. This is a key development for future heat flow and temperature-at-depth calculations

because it modifies the incorporation of the QA relationship for the Texas Gulf Coast and how basement radiogenic heat production is distributed for temperature-at-depth modeling. It is necessary to understand the basement radiogenic heat production distribution for accurate temperature modeling when drilling into the basement, beyond the sedimentary package. The deeper assignments of basement depths in the model incorporated work by others using seismic velocity as a method to map the lithosphere. As new research techniques and data acquisition in many geophysical fields are available, they will improve our understanding of the depth of sediments along the Gulf Coastal Plain and our ability to map temperatures and formation details to much greater depths.

There are measured temperatures of 150 °C in all three counties between 3.0 and 3.5 km depth, therefore reaching the level of potential geothermal electrical production. The next step is to examine formations in these area as possible reservoir opportunities. We suggest to acquire core thermal conductivity measurements of the Pliocene to Cretaceous sediments for these counties and across Texas. These additional data results could improve the heat flow calculation accuracy, as well as, the temperature-at-depth calculations.

References

AAPG, 1978. Basement map of North America, American Association of Petroleum Geologists, Map, Scale 1:5,000,000.

AAPG, 1994. CSDE, COSUNA, and Geothermal Survey, American Association of Petroleum Geologists, Data CD-ROM.

Agrawal, M., Pulliam, J., Sen, M.K. and Gurrola, H., 2015. Lithospheric structure of the Texas-Gulf of Mexico passive margin from surface wave dispersion and migrated Ps receiver functions. *Geochemistry, Geophysics, Geosystems*, *16*(7), pp.2221-2239.

Baker, E.T. 1995. Stratigraphic Nomenclature and geologic sections of the Gulf Coastal Plain of Texas. *USGS,* Open File Report **94-461**, 34 pp.

Batir, J., Richards, M. and Schumann, H., 2018. Reservoir Analysis for Deep Direct-Use Feasibility Study in East Texas. *GRC Transactions*, *42*, p.20.

Blackwell, D.D. 1971. The thermal structure of the continental crust, *in* Heacock, J.G. editor, *The Structure and Physical Properties of the Earth's Crust,* Geophys. Mono. Ser. **14**, 169-184, AGU, Washington D.C.

Blackwell, David D., Negraru, Petru T., and Richards Maria C. 2006. Assessment of the enhanced geothermal system resource base of the United States. *Natural Resources Research* **15-4**, 283-308.

Blackwell, D.D., Steele, J.L., and Carter, L.S. 1991. Heat flow patterns of the North American continent: A discussion of the DNAG geothermal map of North America, *in* Slemmons, D.B., et al., eds., *Neotectonics of North America*: Boulder, Colorado, Geological Society of America, Decade Map Volume 1, p. 423–436.

Blackwell, D., Richards, M., Frone, Z., Batir, J., Ruzo, A., Dingwall, R. and Williams, M., 2011a. *Temperature-at-depth maps for the conterminous US and geothermal resource estimates* (No. GRC1029452). Southern Methodist University Geothermal Laboratory, Dallas, TX (United States).

Blackwell, D.D., Richards, M.C., Frone, Z.S., Batir, J.F., Williams, M.A., Ruzo, A.A. and Dingwall, R.K., 2011b. SMU geothermal laboratory heat flow map of the conterminous United States, 2011. *Supported by Google.org. Available at http://www.smu.edu/geothermal.*

Carter, L.S., Kelley, S.A., Blackwell, D.D., and Naeser, N.D. 1998. Heat flow and thermal history of the Anadarko Basin, Oklahoma: *AAPG Bulletin*, **82**, 291–316.

Čermák, V., Bodri, L. and Rybach, L., 1991. Radioactive heat production in the continental crust and its depth dependence. In *Terrestrial Heat Flow and the Lithosphere Structure* (pp. 23-69). Springer, Berlin, Heidelberg.

Cutright, B.L., 2013. *Finding geothermal resources for project development* (No. Cutright_SMU_GeoConference_2013.pdf). Southern Methodist University Geothermal Laboratory, Dallas, Texas. https://www.osti.gov/servlets/purl/1137016.

Frone, Z.S., Blackwell, D.D., Richards, M.C., Hornbach, M.J. 2015. Heat flow and thermal modeling of the Appalachian Basin, West Virginia. *Geosphere*, **vol. 11-5**, 1279-1290. doi:10.1130/GES01155.1.

Gallardo, J., and Blackwell, D.D. 1999. Thermal structure of the Anadarko Basin: *AAPG Bulletin*, **83**, 333–361.

Galloway, William E. 2008. Depositional Evolution of the Gulf of Mexico Sedimentary Basin. *In* K.J. Hsü, editor: *Sedimentary Basins of the World*, vol 5, *The Sedimentary Basins of the United States and Canada*, Andrew D. Miall. The Netherlands: Elsevier, 505-549.

Gass, T.E., 1982. Geothermal heat pump. In *Bulletin of Geothermal Resources Council.* Davis, Calif.

Hackley, Paul. C. 2012. Geologic Assessment of Undiscovered Conventional Oil and Gas Resources—Middle Eocene Claiborne Group, United States Part of the Gulf of Mexico Basin. *USGS*, Open File Report **2012-1144**, 87 pp. available only at: http://pubs.usgs.gov/of/2012/1144/

Hamlin, H.S. 2009. Ozona sandstone, Val Verde Basin, Texas: Synorogenic stratigraphy and depositional history in a Permian foredeep basin. *AAPG Bulletin*, **vol. 93-5**, 573-594.

Hasterok, D. and J. Webb. 2017. "On the radiogenic heat production of igneous rocks." Geoscience Frontiers 8:919-940. https://doi.org/10.1016/j.gsf.2017.03.006

Horowitz, F.G., Smith, J.D., and Whealton, C.A., 2015. One dimensional conductive geothermal Python code [WWW Document]. https://bitbucket.org/geothermalcode/onedimensionalgeothermalheatconductionmodel.git (accessed May 2017).

Kincade, Sean C. 2018 The Occurrence of the Greta Sandstone, Frio Formation (Late Oligocene), Texas Gulf Coastal Plain. MS Thesis, University of Arkansas, Fayetteville, Arkansas. 75 pp.

Lachenbruch, A.H., 1968, Preliminary geothermal model of the Sierra Nevada: *Journal of Geophysical Research*, **73**, 6977–6989. doi: 10 .1029 /JB073i022p06977.

Lambert, Rebecca B. 2004. Hydrogeology of Webb County, Texas. *USGS*, Open File Report **2004-5022**. Online at: https://pubs.usgs.gov/sir/2004/5022/

McDonnell, Angela, Loucks, R.G., Galloway, W. 2008. Paleocene to Eocene deep-water slope canyons, western Gulf of Mexico: Further insights for the provenance of deep-water offshore Wilcox Group plays. *AAPG Bulletin*, **92-9**, 1169-1189.

McKenna, T.E., and Sharp, J.M. 1998a. Thermal Conductivity of Wilcox and Frio Sandstones in South Texas (Gulf of Mexico Basin). AAPG Bulletin, **80-8**, 1203-1215.

McKenna, T.E. and Sharp, J.M., 1998b. Radiogenic Heat Production in Sedimentary Rocks of the Gulf of Mexico Basin, South Texas. *AAPG bulletin*, **82-3**, 484-496.

NGDS National Geothermal Data System, SMU Node, 2020. Online at: geothermal.smu.edu/GTDA and information regarding content models: https://www.geothermaldata.org/content-models/data-interchange-content-models.

Pitman, J.K. and Rowan, E.R. 2012. Temperature and petroleum generation history of the Wilcox Formation, Louisiana, *USGS,* Open File Report **2012-1046**, 51 pp.

Richards, Maria and David Blackwell, 2012, Developing Geothermal Energy in Texas: Mapping the Temperatures and Resources, GCAGS and GC-SEPM 62nd Annual Convention, Austin, Texas, 21-24 October 2012, Pages 351-363.

Richards, Maria, David Blackwell, Mitchell Williams, Zachary Frone, Ryan Dingwall, Joseph Batir, and Cathy Chickering. 2012. "Proposed Reliability Code for Heat Flow Sites." *Geothermal Resources Council Trans.* 36: 211-218.

Roy, R.F., Blackwell, D.D., and Birch, F. 1968. Heat generation of plutonic rocks and continental heat flow provinces. *Earth and Planetary Science Letters*, **5**, 1–12. doi:10.1016 /S0012-821X (68)80002 -0.

Rybach, Ladislaus, 2020. Heat Flow Determination with Geothermal Heat Pump Data, GRC Transactions, Vol 44, 11 pp.

Smith, Jared. 2016. Analytical and geostatistical heat flow modeling for geothermal resource reconnaissance applied in the Appalachian Basin. PhD Dissertation, Cornell University, Ithaca, NY.

Smith, J.D. and Horowitz, F.G., 2016. Memo 8: Thermal Model Methods and Well Database Organization in GPFA-AB, *in:* January 2017 upload of Jordan, Teresa E. et al., Final Report: Low Temperature Geothermal Play Fairway Analysis for the Appalachian Basin. pp. 202–234. https://gdr.openei.org/files/899/GPFA-AB_Final_Report_with_Supporting_Documents.pdf

Stutz, George R., Shope, Elaina, Aguirre, Gloria Andrea, Batir, Joseph, Frone, Zachary, Williams, Mitchell, Reber, Timothy J., Whealton, Calvin A., Smith, Jared D., Richards, Maria C., Blackwell, David D., Tester, Jefferson W., Stedinger, Jery R. and Jordan, Teresa E. 2015. Geothermal energy characterization in the Appalachian Basin of New York and Pennsylvania. *Geosphere*, **11**, no. 5, 1291-1304.

Turchi, C.S., McTigue, J.D.P., Akar, S., Beckers, K.J., Richards, M., Chickering, C., Batir, J., Schumann, H., Tillman, T. and Slivensky, D., 2020. *Geothermal Deep Direct Use for Turbine Inlet Cooling in East Texas* (No. NREL/TP-5500-74990). National Renewable Energy Lab. (NREL), Golden, CO (United States). DOI: 10.2172/1602704

Warwick, Peter D. 2017. Geologic Assessment of Undiscovered Conventional Oil and Gas Resources in the Lower Paleogene Midway and Wilcox Groups, and the Carrizo Sand of the Claiborne Group, of the Northern Gulf Coast Region. *USGS*, Open File Report **2017-1111**, 67 pp. Online at: https://doi.org/10.3133/ofr20171111

Welldatabase, 2020. Public geologic formation top data collection, accessed through Lite plan subscription. Online at: https://welldatabase.com/

Zafar, S.D. and Cutright, B.L., 2014. Texas' geothermal resource base: a raster-integration method for estimating in-place geothermal-energy resources using ArcGIS. *Geothermics*, *50*, pp.148-154.

Appendix A: Thermal Conductivity Lithology Models

Below are the thermal conductivity lithology models used for well site thickness weighted thermal conductivity calculations and temperature-at-depth modeling. The assumed thickness is the starting thickness for each formation, before depth scaling to fit the lithology section to the total sediment thickness. Lithology notes states where formation thickness values come from, which is visible in the supplementary Excel file, “lithologypages.xlsx”. The last table is the Pitman and Rowan (2012) thermal conductivity values that were used for Webb and Jackson Counties’ lithology models.

Table A- 1. North Crockett County Thermal Conductivity Lithology Model.

Age	unit/formation	Unit	Column Min m	Min Thickness m	Max Thickness m	Min(avg) Thickness m	Max(avg) Thickness m	Assumed Thickness m	Thickness Std. Dev. m	Detailed Rock type	Lithology Notes	Thermal Conductivity W/m*K	Formation Top Depth m
Quaternary	Quaternary	UNCON	0	0	15	0	15	15	0		Cosuna, 1994;	2.77	0
Cretaceous	Edwards Limestone	LS	0	75	155	75	155	95	0		Cosuna, 1994;	2.9	15
	Paluxy Sandstone	SS	0	75	155	75	155	95	0		Cosuna, 1994;	3	110
Permian (Guadalupian)	Dewey Lake Fm	SS	0	25	80	0	80	0	0		Cosuna, 1994;	2.8	205
	Rustler Fm *Combination SALT to the Yates	EVAP	0	30	150	30	150	150	0		Cosuna, 1994;	4.65	205
	Salado Fm	EVAP	0	215	670	215	670	0	0		Cosuna, 1994;	4.65	355
	Tansill	EVAP	0	23	40	23	40	0	0		Cosuna, 1994;	4.65	355
	Yates	SS	0	37	100	37	100	100	0		Cosuna, 1994;	2.8	355
	Seven Rivers	EVAP	0	150	200	150	200	151	0		Cosuna, 1994;	4.65	455
	Queen	SS/EVA	0	50	250	100	200	90	0		Cosuna, 1994;	3.2	606
	Grayburg	LS	0	40	250	75	100	50	0		Cosuna, 1994;	2.9	696
	San Andres Dolomite	DOL	0	100	500	100	300	450	0		Cosuna, 1994;	3.3	746
	Glorieta Sandstone	SS	0	0	366	0	366	0	0		Cosuna, 1994;	2.8	1196
Lower Permian (Leonardia	Clearfork Group (Includes Spraberry and Dean)	LS/SH	0	100	750	200	600	400	0		Cosuna, 1994;	2.35	1196
	Spraberry	SH/SS	0	100	750	200	600	225	0		Cosuna, 1994;	2.3	1596
	Dean	SS/LS	0	100	750	200	600	175	0		Cosuna, 1994;	2.85	1821
Lower Permian (Wolfcamp	Wolfcamp Group	LS/SH	0	0	2000	250	1000	620	0		Cosuna, 1994;	2.35	1996
Carboniferous	Cisco Limestone (Upper Ozona Sequence)	LS	0	76	173	76	173	150	0		Hamlin, 2009	2.9	2616
	Middle Ozona (Slope Facies)	SH	0	0	130	0	130	97	0		Hamlin, 2009	2.5	2766
	Lower Ozona (Turbidite Sheets)	SH/SS	0	100	150	100	150	137	0		Hamlin, 2009 -	2.05	2863
	Sonora	SH	0	100	305	100	305	180	0		Hamlin, 2009	1.6	3000
	Strawn	LS	0	0	80	0	80	40	0		COSUNA, 1994	2.5	3180
	Barnett Sh	SH	0	0	150	30	150	75	0		COSUNA, 1994	1.6	3220
	Mississppian Lime	LS	0	0	136	70	136	120	0		COSUNA, 1994	2.5	3295
Devonian	Woodford Sh	SH	0	0	186	0	100	85	0		COSUNA, 1994	1.6	3415
	Thirtyone Fm.	LS	0	0	300	0	150	50	0		COSUNA, 1994	2.5	3500
	Wristen Fm.	LS/SH	0	0	120	30	60	45	0		COSUNA, 1994	2	3550
	Fusselman Dol.	DOL	0	0	300	30	150	50	0		COSUNA, 1994	3	3595
	Montoya Dol.	DOL	0	0	136	0	100	40	0		COSUNA, 1994	3	3645
	Simpson Grp	LS/SH	0	0	530	100	500	100	0		COSUNA, 1994	2	3685
	Ellenburger Dol.	DOL	0	200	500	200	500	300	0		COSUNA, 1994	3	3785
	Cambrian SS	SS	0	0	100	0	100	30	0		COSUNA, 1994	2.8	4085
	total							4115					4115
Additional Notes:	For Conductivity values: Red = Pitman and Rowan, 2012; Blue = Frone et al., 2015; Black = Carter et al., 1998 and Gallardo and Blackwell, 1999; Yellow = new average from Frone et al., Carter et al., and Gallardo and Blackwell for this study												

Table A- 2. South Crockett County Thermal Conductivity Lithology Model.

Age	unit/formation	Unit	Column Min m	Min Thickness m	Max Thickness m	Min(avg) Thickness m	Max(avg) Thickness m	Assumed Thickness m	Thickness Std. Dev. m	Detailed Rock type	Lithology Notes	Thermal Conductivity W/m*K	Formation Top Depth m
Quaternary	Quaternary	UNCON	0	0	15	0	15	15	0		Cosuna, 19	2.77	0
Cretaceous	Edwards Limestone	LS	0	75	155	75	155	140	0		Cosuna, 19	2.9	15
	Paluxy Sandstone	SS	0	75	155	75	155	140	0		Cosuna, 19	3	155
Permian (Guadalupian)	Dewey Lake Fm	SS	0	25	80	0	80	0	0		Cosuna, 19	2.8	295
(0 to 650 m)	Rustler Fm *Combination SALT to the Yates	EVAP	0	30	150	30	150	0	0		Cosuna, 19	4.65	295
	Salado Fm	EVAP	0	215	670	215	670	0	0		Cosuna, 19	4.65	295
	Tansill	EVAP	0	23	40	23	40	0	0		Cosuna, 19	4.65	295
	Yates	SS	0	37	100	37	100	0	0		Cosuna, 19	2.8	295
	Seven Rivers	EVAP	0	150	200	150	200	0	0		Cosuna, 19	4.65	295
	Queen	SS/EVAP	0	50	250	100	200	90	0		Cosuna, 19	3.2	295
	Grayburg	LS	0	40	250	75	100	50	0		Cosuna, 19	2.9	385
	San Andres Dolomite	DOL	0	100	500	100	300	325	0		Cosuna, 19	3.3	435
	Glorieta Sandstone	SS	0	0	366	0	366	0	0		Cosuna, 19	2.8	760
Lower Permian (Leonardian)	Clearfork Group (Includes Spraberry and Dean)	LS/SH	0	100	750	200	600	240	0		Cosuna, 19	2.35	760
(0 to 610, avg. 600)	Spraberry	SH/SS	0	100	750	200	600	225	0		Cosuna, 19	2.3	1000
	Dean	SS/LS	0	30	750	30	100	100	0		Cosuna, 19	2.85	1225
Lower Permian (Wolfcampian)	Wolfcamp Group	LS/SH	0	0	2000	250	1000	500	0		Cosuna, 19	2.35	1325
Carboniferous	Cisco Limestone (Upper Ozona Sequence)	LS	0	133	173	133	173	147	0		Hamlin, 20	2.9	1825
	Upper Ozona Sandstone	SS	0	23	70	23	70	50	0		Hamlin, 20	2.8	1972
	Middle Ozona Sequence (Channels and Turbidites)	SS/SH	0	90	130	90	130	117	0		Hamlin, 20	2.5	2022
	Lower Ozona (Turbidite Sheets)	SH/SS	0	120	154	120	154	130	0		Hamlin, 20	2.05	2139
	Sonora	SH	0	100	2750	335	2750	1300	0		Hamlin, 20	1.6	2269
	Strawn	LS	0	0	80	0	80	70	0		COSUNA, 1	2.5	3569
	Barnett Sh	SH	0	0	150	30	150	70	0		COSUNA, 1	1.6	3639
	Mississppian Lime	LS	0	0	136	70	136	30	0		COSUNA, 1	2.5	3709
Devonian	Woodford Sh	SH	0	0	186	0	100	40	0		COSUNA, 1	1.6	3739
	Thirtyone Fm.	LS	0	0	300	0	150	80	0		COSUNA, 1	2.5	3779
	Wristen Fm.	LS/SH	0	0	120	30	60	45	0		COSUNA, 1	2	3859
	Fusselman Dol.	DOL	0	0	300	30	70	50	0		COSUNA, 1	3	3904
	Sylvan Shale	SH	0	8	40	8	40	25	0		COSUNA, 1	1.6	3954
	Montoya Dol.	DOL	0	0	136	0	100	30	0		COSUNA, 1	3	3979
	Simpson Grp	LS/SH	0	0	530	100	500	66	0		COSUNA, 1	2	4009
	Ellenburger Dol.	DOL	0	200	500	200	500	315	0		COSUNA, 1	3	4075
	Cambrian SS	SS	0	0	100	0	100	30	0		COSUNA, 1	2.8	4390
	total							4420					4420
Additional Notes:	For Conductivity values: Red = Pitman and Rowan, 2012; Blue = Frone et al., 2015; Black = Carter et al., 1998 and Gallardo and Blackwell, 1999; Yellow = new average from Frone et al., Carter et al., and Gallardo and Blackwell for this study												

Table A- 3. North Webb County Thermal Conductivity Lithology Model.

Age	unit/formation	Unit	Column Min m	Min Thickness m	Max Thickness m	Min(avg) Thickness m	Max(avg) Thickness m	Assumed Thickness m	Thickness Std. Dev. m	Detailed Rock type	Lithology Notes	Thermal Conductivity W/m*K	Formation Top Depth m
Quaternary	Quaternary	UNCON	0	0	15	0	15	15	0		COSUNA, 19	2.77	0
Eocene	Laredo Formation (middle Eocene)	SED	0	0	292	100	292	150	0		Baker, 1994	2.6	15
	El Pico Clay	SH	0	0	305	268	292	275	0		Baker, 1994	2	165
	Queen City Sand	SED	0	0	107	61	107	80	0		Lambert, 200	2.6	440
	Bigford Formation	SS/SH	0	0	305	150	250	250	0		Baker, 1994	2.6	520
	Carrizo Sand	SS	35	35	305	150	250	210	0		Baker, 1994	2.77	770
	Indio formation / Wilcox Group	SS/SLT/SH	231	231	646	235	650	475	0		Baker, 1994	2.3	980
Paleocene	Midway Group	SH	85	85	245	85	245	165	0		Baker, 1994	2	1455
Upper Cretaceous	Escondido Formation	SS/SH	400	400	660	400	660	425	0		Baker, 1994	2.3	1620
	Olmos Formation	SS	244	244	305	244	305	280	0		Baker, 1994	2.3	2045
	Taylor Marl / San Miguel Formation	SS/SH/LS	135	135	195	135	195	160	0		Baker, 1994	2.2	2325
	Taylor Marl / Upson Clay	SS/SH/LS	158	158	183	158	183	171	0		Baker, 1994	2.2	2485
	Austin Group	SH/LS	207	207	256	207	256	232	0		Baker, 1994	2.7	2656
	Eagle Ford Shale	SH/LS	110	110	195	110	195	160	0		Baker, 1994	2.35	2888
	Buda Limestone	LS	36	36	49	36	49	43	0		Baker, 1994	2.46	3048
	Del Rio Clay	SH	30	30	30	30	30	30	0		Baker, 1994	2	3091
Lower Cretaceous	Georgetown Limestone	LS	85	85	146	85	146	98	0		Baker, 1994	2.6	3121
	Fredericksburg Group	LS	159	159	415	159	415	225	0		Baker, 1994	2.6	3219
	Glen Rose Limeston	LS	36	36	342	36	342	122	0		Baker, 1994	2.6	3444
	Pearsall Formation	SS/LS	36	36	183	36	183	85	0		Baker, 1994	2.4	3566
	Sligo Formation	LS	24	24	820	50	200	300	0		Baker, 1994	2.4	3651
	Hosston Formation	SED	0	0	600	0	600	300	0		COSUNA, 19	2.3	3951
	Cotton Valley	SED	0	0	366	0	366	300	0		COSUNA, 19	2.3	4251
	Buckner Formation	EVAP	0	0	120	0	120	60	0		COSUNA, 19	4.65	4551
	Smackover Formation	LS	0	0	300	0	300	150	0		COSUNA, 19	2.56	4611
	Norphlet Formation	SS	0	0	35	0	35	35	0		COSUNA, 19	2.2	4761
	total							4796					4796
Additional Notes:	For Conductivity values: Red = Pitman and Rowan, 2012; Blue = Frone et al., 2015; Black = Carter et al., 1998 and Gallardo and Blackwell, 1999; Yellow = new average from Frone et al., Carter et al., and Gallardo and Blackwell for this study												

Table A- 4. Southwest Webb County Thermal Conductivity Lithology Model.

Age	unit/formation	Unit	Column Min m	Min Thickness m	Max Thickness m	Min(avg) Thickness m	Max(avg) Thickness m	Assumed Thickness m	Thickness Std. Dev. m	Detailed Rock type	Lithology Notes	Thermal Conductivity W/m*K	Formation Top Depth m
Quaternary	Quaternary	UNCON	0	0	15	0	15	15	0		COSUNA, 199	2.77	0
Eocene	Jackson Group (Includes Frio and Vicksburg)	SH/SS	0	0	1000	0	500	0	0		Lambert, 200	2.23	15
	Yegua	SS	0	0	365	0	350	300	0		Lambert, 200	2.6	15
	Laredo Formation (middle Eocene)	SED	0	0	390	0	350	250	0		Baker, 1994 &	2.6	315
	El Pico Clay	SH	50	50	300	50	300	275	0		Baker, 1994 &	2	565
	Queen City Sand	SED	102	102	305	102	305	250	0		Lambert, 200	2.6	840
	Bigford Formation	SS/SH	293	293	457	293	457	350	0		Baker, 1994 &	2.6	1090
	Reklaw Formation	SH	0	0	163	0	163	100	0		Lambert, 200	2.15	1440
Paleocene	Carrizo Sand	SS	244	244	355	244	355	305	0		Baker, 1994 &	2.77	1540
Upper Cretaceous	Indio formation / Wilcox Group	SS	575	575	1500	575	900	700	0		Baker, 1994 -	2.3	1845
	Midway Group	SH	244	244	293	244	293	270	0		Baker, 1994	2	2545
	Escondido Formation	SS/SH	512	512	650	512	650	600	0		Baker, 1994	2.3	2815
	Olmos Formation	SS	170	170	305	170	305	250	0		Baker, 1994	2.3	3415
	Taylor Marl / San Miguel Formation	SS/SH/LS	135	135	195	135	195	160	0		Baker, 1994	2.2	3665
	Taylor Marl / Upson Clay	SS/SH/LS	158	158	183	158	183	171	0		Baker, 1994	2.2	3825
	Austin Group	SH/LS	207	207	256	207	256	256	0		Baker, 1994	2.7	3996
	Eagle Ford Shale	SH/LS	110	110	195	110	195	195	0		Baker, 1994	2.35	4252
Lower Cretaceous	Buda Limestone	LS	36	36	49	36	49	43	0		Baker, 1994	2.46	4447
	Del Rio Clay	SH	30	30	30	30	30	30	0		Baker, 1994	2	4490
	Georgetown Limestone	LS	85	85	146	85	146	85	0		Baker, 1994	2.6	4520
	Fredericksburg Group	LS	159	159	415	159	415	250	0		Baker, 1994	2.6	4605
	Glen Rose Limeston	LS	36	36	342	36	342	61	0		Baker, 1994	2.6	4855
	Pearsall Formation	SS/LS	36	36	183	36	183	85	0		Baker, 1994	2.4	4916
	Sligo Formation	LS	24	24	820	50	200	300	0		Baker, 1994 &	2.4	5001
	Hosston Formation	SED	0	0	600	0	600	300	0		COSUNA, 199	2.3	5301
	Cotton Valley	SED	0	0	366	0	366	300	0		COSUNA, 199	2.3	5601
	Buckner Formation	EVAP	0	0	120	0	120	60	0		COSUNA, 199	4.65	5901
	Smackover Formation	LS	0	0	300	0	300	150	0		COSUNA, 199	2.56	5961
	Norphlet Formation	SS	0	0	35	0	35	35	0		COSUNA, 199	2.2	6111
	total							6146					6146
Additional Notes:	For Conductivity values: Red = Pitman and Rowan, 2012; Blue = Frone et al., 2015; Black = Carter et al., 1998 and Gallardo and Blackwell, 1999; Yellow = new average from Frone et al., Carter et al., and Gallardo and Blackwell for this study												

Table A- 5. Southcentral Webb County Thermal Conductivity Lithology Model.

Age	unit/formation	Unit	Column Min m	Min Thickness m	Max Thickness m	Min(avg) Thickness m	Max(avg) Thickness m	Assumed Thickness m	Thickness Std. Dev. m	Detailed Rock type	Lithology Notes	Thermal Conductivity W/m*K	Formation Top Depth m
Quaternary	Quaternary	UNCON	0	0	15	0	15	15	0		COSUNA, 19	2.77	0
Eocene	Jackson Group (Includes Frio and Vicksburg)	SH/SS	0	0	1000	0	500	200	0		Lambert, 200	2.23	15
	Yegua	SS	0	0	365	0	350	225	0		Lambert, 200	2.6	215
	Laredo Formation (middle Eocene)	SED	0	0	390	0	350	250	0		Baker, 1994	2.6	440
	El Pico Clay	SH	50	50	300	50	300	275	0		Baker, 1994	2	690
	Queen City Sand	SED	102	102	305	102	305	250	0		Lambert, 200	2.6	965
	Bigford Formation	SS/SH	293	293	457	293	457	350	0		Baker, 1994	2.6	1215
	Reklaw Formation	SH	0	0	163	0	163	100	0		Lambert, 200	2.15	1565
Paleocene	Carrizo Sand	SS	244	244	355	244	355	305	0		Baker, 1994	2.77	1665
Upper Cretaceous	Indio formation / Wilcox Group	SS	575	575	1500	575	900	700	0		Baker, 1994	2.3	1970
	Midway Group	SH	244	244	293	244	293	270	0		Baker, 1994	2	2670
	Escondido Formation	SS/SH	512	512	650	512	650	600	0		Baker, 1994	2.3	2940
	Olmos Formation	SS	170	170	305	170	305	250	0		Baker, 1994	2.3	3540
	Taylor Marl / San Miguel Formation	SS/SH/LS	135	135	195	135	195	160	0		Baker, 1994	2.2	3790
	Taylor Marl / Upson Clay	SS/SH/LS	158	158	183	158	183	171	0		Baker, 1994	2.2	3950
	Austin Group	SH/LS	207	207	256	207	256	256	0		Baker, 1994	2.7	4121
	Eagle Ford Shale	SH/LS	110	110	195	110	195	195	0		Baker, 1994	2.35	4377
Lower Cretaceous	Buda Limestone	LS	36	36	49	36	49	43	0		Baker, 1994	2.46	4572
	Del Rio Clay	SH	30	30	30	30	30	30	0		Baker, 1994	2	4615
	Georgetown Limestone	LS	85	85	146	85	146	85	0		Baker, 1994	2.6	4645
	Fredericksburg Group	LS	159	159	415	159	415	250	0		Baker, 1994	2.6	4730
	Glen Rose Limeston	LS	36	36	342	36	342	61	0		Baker, 1994	2.6	4980
	Pearsall Formation	SS/LS	36	36	183	36	183	85	0		Baker, 1994	2.4	5041
	Sligo Formation	LS	24	24	820	50	200	300	0		Baker, 1994	2.4	5126
	Hosston Formation	SED	0	0	600	0	600	300	0		COSUNA, 19	2.3	5426
	Cotton Valley	SED	0	0	366	0	366	300	0		COSUNA, 19	2.3	5726
	Buckner Formation	EVAP	0	0	120	0	120	60	0		COSUNA, 19	4.65	6026
	Smackover Formation	LS	0	0	300	0	300	150	0		COSUNA, 19	2.56	6086
	Norphlet Formation	SS	0	0	35	0	35	35	0		COSUNA, 19	2.2	6236
	total							6271					6271
Additional Notes:	For Conductivity values: Red = Pitman and Rowan, 2012; Blue = Frone et al., 2015; Black = Carter et al., 1998 and Gallardo and Blackwell, 1999; Yellow = new average from Frone et al., Carter et al., and Gallardo and Blackwell for this study												

Table A- 6. Southeast Webb County Thermal Conductivity Lithology Model.

Age	unit/formation	Unit	Column Min m	Min Thickness m	Max Thickness m	Min(avg) Thickness m	Max(avg) Thickness m	Assumed Thickness m	Thickness Std. Dev. m	Detailed Rock type	Lithology Notes	Thermal Conductivity W/m*K	Formation Top Depth m
Quaternary	Quaternary	UNCON	0	0	15	0	15	15	0		COSUNA, 19	2.77	0
Eocene	Jackson Group (Includes Frio and Vicksburg)	SH/SS	0	0	1000	0	500	500	0		Lambert, 200	2.23	15
	Yegua	SS	0	0	365	0	350	225	0		Lambert, 200	2.6	515
	Laredo Formation (middle Eocene)	SED	0	0	390	0	350	152	0		Baker, 1994	2.6	740
	El Pico Clay	SH	50	50	300	50	300	275	0		Baker, 1994	2	892
	Queen City Sand	SED	102	102	305	102	305	152	0		Lambert, 200	2.6	1167
	Bigford Formation	SS/SH	293	293	457	293	457	350	0		Baker, 1994	2.6	1319
	Reklaw Formation	SH	0	0	163	0	163	100	0		Lambert, 200	2.15	1669
Paleocene	Carrizo Sand	SS	244	244	355	244	355	305	0		Baker, 1994	2.77	1769
Upper Cretaceous	Indio formation / Wilcox Group	SS	575	575	1500	575	900	700	0		Baker, 1994	2.3	2074
	Midway Group	SH	244	244	293	244	293	270	0		Baker, 1994	2	2774
	Escondido Formation	SS/SH	512	512	650	512	650	600	0		Baker, 1994	2.3	3044
	Olmos Formation	SS	170	170	305	170	305	250	0		Baker, 1994	2.3	3644
	Taylor Marl / San Miguel Formation	SS/SH/LS	135	135	195	135	195	160	0		Baker, 1994	2.2	3894
	Taylor Marl / Upson Clay	SS/SH/LS	158	158	183	158	183	171	0		Baker, 1994	2.2	4054
	Austin Group	SH/LS	207	207	256	207	256	256	0		Baker, 1994	2.7	4225
	Eagle Ford Shale	SH/LS	110	110	195	110	195	195	0		Baker, 1994	2.35	4481
Lower Cretaceous	Buda Limestone	LS	36	36	49	36	49	43	0		Baker, 1994	2.46	4676
	Del Rio Clay	SH	30	30	30	30	30	30	0		Baker, 1994	2	4719
	Georgetown Limestone	LS	85	85	146	85	146	85	0		Baker, 1994	2.6	4749
	Fredericksburg Group	LS	159	159	415	159	415	250	0		Baker, 1994	2.6	4834
	Glen Rose Limeston	LS	36	36	342	36	342	61	0		Baker, 1994	2.6	5084
	Pearsall Formation	SS/LS	36	36	183	36	183	85	0		Baker, 1994	2.4	5145
	Sligo Formation	LS	24	24	820	50	200	300	0		Baker, 1994	2.4	5230
	Hosston Formation	SED	0	0	600	0	600	300	0		COSUNA, 19	2.3	5530
	Cotton Valley	SED	0	0	366	0	366	300	0		COSUNA, 19	2.3	5830
	Buckner Formation	EVAP	0	0	120	0	120	60	0		COSUNA, 19	4.65	6130
	Smackover Formation	LS	0	0	300	0	300	150	0		COSUNA, 19	2.56	6190
	Norphlet Formation	SS	0	0	35	0	35	35	0		COSUNA, 19	2.2	6340
	total							6375					6375
Additional Notes:	For Conductivity values: Red = Pitman and Rowan, 2012; Blue = Frone et al., 2015; Black = Carter et al., 1998 and Gallardo and Blackwell, 1999; Yellow = new average from Frone et al., Carter et al., and Gallardo and Blackwell for this study												

Table A- 7. Jackson County Thermal Conductivity Lithology Model.

Age	unit/formation	Unit	Column Min m	Min Thickness m	Max Thickness m	Min(avg) Thickness m	Max(avg) Thickness m	Assumed Thickness m	Thickness Std. Dev. m	Detailed Rock type	Lithology Notes	Thermal Conductivity W/m*K	Formation Top Depth m
Quaternary	Quaternary	UNCON	0	0	0	0	0	15	0		COSUNA, 199	2.77	0
Pre-Miocene	Pre-Miocene	SS	0	0	0	0	0	305	0		COSUNA, 199	2.6	15
Upper/Middle Miocene	Lagarto / Oakville	SS/SH	0	0	0	0	0	457	0		COSUNA, 199	2.3	320
Lower Miocene	Catahoula	SED	107	107	265	107	265	183	52		McDonnell et	2.3	777
Lower Miocene	Anahuac	SH	203	203	351	203	351	277	74		McDonnell et	2.24	960
Upper Oligocene	Frio (Top Section Greta)	SS	31	31	985	31	985	640	370		McDonnell et	2.24	1237
Lower Oligocene	Vicksburg	SH	116	116	291	116	291	229	30		McDonnell et	2.3	1877
Upper Eocene	Jackson Group	SS/SH	207	207	1604	207	1604	889	495		McDonnell et	2.23	2105
	Yegua	SS/SH	21	21	1079	21	1079	317	327		McDonnell et	2.1	2995
	Weches	SH	219	219	219	219	219	219	0		McDonnell et	2.05	3311
	Queen City	SS	456	456	458	456	458	457	1		McDonnell et	2.3	3531
Upper Cretaceous	Wilcox	SS/SH	219	219	219	219	219	1067	0		McDonnell et	2.15	3988
Cretaceous	Cretaceous Abyssal Plain Shale	SH	0	0	0	0	0	1219	0		COSUNA, 199	1.9	5054
	total							6274					6274
Additional Notes:	**For Conductivity values: Red = Pitman and Rowan, 2012; Blue = Frone et al., 2015; Black = Carter et al., 1998 and Gallardo and Blackwell, 1999; Yellow = new average from Frone et al., Carter et al., and Gallardo and Blackwell for this study**												

Table A- 8. Pitman and Rowan (2012) formation lithologies and physical and thermal properties as defined in models of Louisiana wells. Thermal conductivity source for Webb and Jackson Counties.

Model	Lithology	Thermal cond.	Thermal cond.	Thermal cond.	Heat capacity	Heat capacity
Unit		at 20° C	at 100° C	Anisotropy	at 20° C	at 100° C
Name	(percent)	($Wm^{-1}K^{-1}$)	($Wm^{-1}K^{-1}$)	(Fraction)	(kcal/kg/K)	(kcal/kg/K)
PLEISTOCENE	65 SS/30 SLT/05 SH	2.77	2.42	1.18	0.187	0.221
PLIOCENE	50 SS/40 SLT/10 SH	2.61	2.32	1.22	0.191	0.227
UPPER MIOCENE	20 SS/60 SLT/20 SH	2.30	2.13	1.30	0.199	0.239
MIDDLE MIOCENE	15 SS/55 SLT/30 SH	2.24	2.09	1.33	0.201	0.242
LOWER MIOCENE	20 SS/55 SLT/25 SH	2.30	2.12	1.31	0.199	0.239
FRIO	15 SS/55 SLT/30 SH	2.24	2.09	1.33	0.201	0.242
VICKSBURG	20 SS/55 SLT/25 SH	2.30	2.12	1.31	0.199	0.239
JACKSON	15 SS/50 SLT/35 SH	2.23	2.08	1.34	0.202	0.243
CLAIBORNE	10 SS/35 SLT/55 SH	2.15	2.02	1.39	0.205	0.248
WILCOX	20 SS/60 SLT/20 SH	2.30	2.13	1.30	0.199	0.239
MIDWAY	10 SLT/90 SH	2.00	1.92	1.48	0.212	0.256
NAVARRO	15 SLT/65 SH/10 CARB/10 CHALK	2.18	2.05	1.39	0.208	0.249
AUSTIN	5 SLT/5 SH/90 CHALK	2.77	2.46	1.13	0.198	0.228
EAGLEFORD	10 SLT/90 SH	2.00	1.92	1.48	0.212	0.256
TUSCALOOSA	35 SS/20 SLT/45 SH	2.41	2.19	1.32	0.198	0.238
WASHITA	5 SLT/30 SH/65 CARB	2.54	2.34	1.23	0.201	0.234
FREDRICKSBURG	5 SLT/10 SH/75 CARB/10 EVAP	2.90	2.60	1.14	0.197	0.226
SLIGO	25 SS/15 SLT/15 SH/45 CARB	2.67	2.40	1.19	0.194	0.228
COTTON VALLEY	15 SS/40 SLT/20 SH/20 CARB/5 EVAP	2.52	2.30	1.26	0.198	0.235
SMACKOVER	5 SS/95 CARB	2.84	2.56	1.10	0.194	0.222

[ss, sandstone; slt, siltstone; sh, shale; carb, carbonate; evap, evaporite; T-cond., thermal conductivity; kg/m3, kilogram per cubic meter; $Wm^{-1}K^{-1}$, watts per meter kelvin; kcal/kg/K, kilocalories per kilogram per kelvin]

Appendix B: White Paper Proposals to BEG related to this project

The following proposals are developed based on the research and results of this three county temperature-at-depth mapping project. There continues to be a need for additional understanding of basic parameters for heat flow calculations and expansion of a one-county review of radiogenic heat production. Although these are commonly used parameters for multiple industries, the standard has been to just use averages or values from other studies. This project shows the amount of additional error possible and the compounding of such errors as the values are then used to calculate deeper values. The ability to evaluate the cost of a project is then compounded as the depths necessary to drill to become more variable and unpredictable.

Proposal - Review current oil and gas well log Bottom-Hole Temperatures

Proposal - Thermal Conductivity Database

Proposal - Combine Seismic Data and Heat Flow Data to examine Radiogenic Heat Production

Proposal: Review current oil and gas well log Bottom-Hole Temperatures

Maria Richards and Joseph Batir
SMU Geothermal Laboratory, Dallas, Texas
mrichard@smu.edu 214-768-1975

September 23, 2020

The oil and gas industry improved their drilling time and changed their techniques significantly over the past 20 years. These include changes in the amount and type of drilling fluid, the timeframe between drilling and logging, the depth of wells and length of horizontals, and improvements in logging tools. All of these changes impact the temperature measurements of the borehole, submitted as BHT, or bottom-hole temperature and/or a maximum temperature recorded.

The borehole temperature is the foundation of heat flow studies as the most commonly measured parameter. Other common parameters for resource evaluation are thermal conductivity, radiogenic heat production, reservoir pressure, and fluid type and flow rates. Therefore, understanding the input data of current temperatures is necessary to reduce modeling errors that lead to over or under prediction of the Texas thermal resources.

The current SMU Geothermal Laboratory research, which is part of the Texas GEO project, highlights newer wells drilled between 2000 and 2007 (Figures 1 and 2), from data collected by MLKay Technologies for the SMU National Geothermal Data System project. These newer BHT sites show over a broad area in Southeast Webb County, the newest temperatures as being generally cooler and more tightly constrained than the full dataset from the BEG IGOR dataset, which goes back to the 1960s.

The heat flow community commonly uses the Harrison Correction (Blackwell and Richards, 2004; Richards and Blackwell, 2012), which is based on a set temperature increase or decrease according to the well depth for oil and gas wells. Corrections are considered necessary, as temperatures in the past were known to be generally too cool for the measured depth because of drilling influence impacting the borehole. Therefore, if drilling techniques are changing the standard BHT value, then knowing how to correct the newest data points is of utmost importance for accurate calculations of temperatures at depth and deeper geothermal resource evaluations.

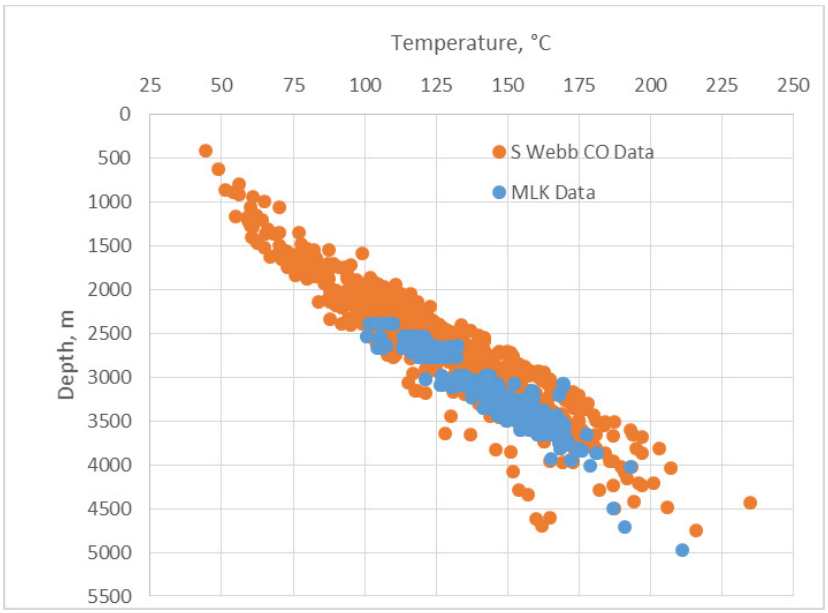

Figure 1. Temperature-depth plot of oil and gas wells from Southeast Webb County. The orange data are older well log temperatures (pre 2000) and the blue data are newer well log temperatures (post 2000).

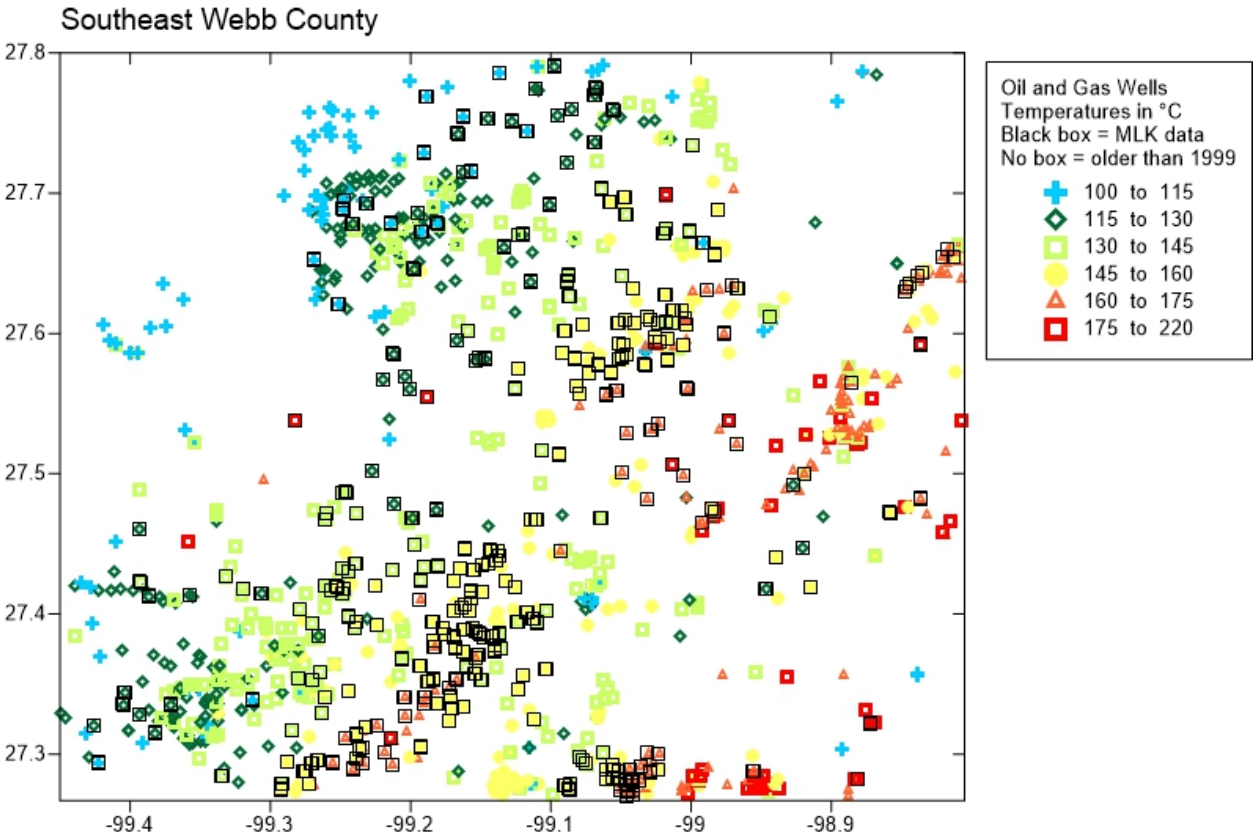

Figure 2. Surface view of Southeast Webb County well temperatures. The post 2000 well data from MLK Technologies, are highlighted with a black box around sites, and the older (pre 2000) well data from

BEG IGOR database are plotted only as temperature (°C) value. Overall the distribution of the smaller MLK well sites are distributed centrally with similar or cooler values for the surrounding area.

The significant increase in horizontal drilling provides an additional necessary review of well temperature data to determine if the maximum recorded values are reaching an equilibrium state, or close to it near the depth where the well changes from vertical to horizontally drilled. As Figure 3 shows a temperature log of a Webb County Eagle Ford well drilled in 2017. The coldest point is at the end of the horizontal (most recently drilled portion) and the warmest at the shallowest portion of the well (253°F @ 6529 ft [123°C @1991 m]), which puts this data point as one of the hottest temperatures for this depth in Webb County. Without understanding the scenario of the borehole, the temperature is corrected with an increase of ~10°C using the Harrison Correction. This increase of 10°C may not seem significant until the gradient is used to calculate the heat flow, which is used to determine expected temperatures at 6 km. The 10°C temperature difference becomes ~30°C hotter at 6 km. Whether the resource evaluation is for geothermal energy production or finding the windows for oil and gas maturation, this amount of difference does change the usable outcome of the related reservoir.

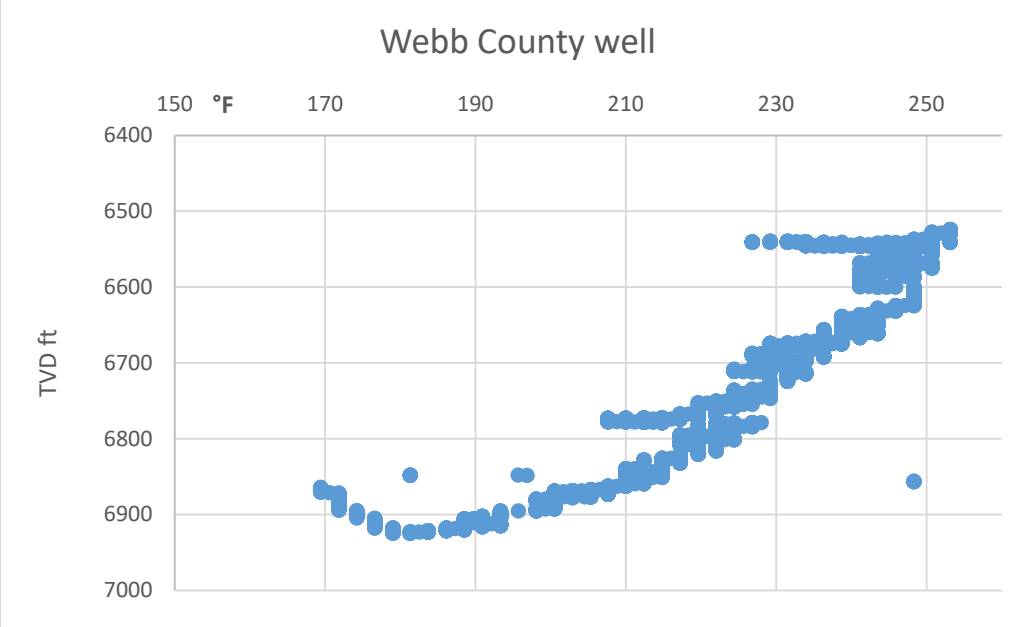

Figure 3. Webb County Eagle Ford well log measuring temperature from the longest lateral point (at ~170°F) to the main well (~253°F).

How the changes in drilling and logging tools impact the in situ well temperatures has not been recently researched. The proposed project is therefore to improve the understanding of temperatures collected from well logs between 2010 and 2020. To achieve this goal: 1) Acquire well logs (LAS preferred) from companies and the Railroad commission drilled in the past 10 years. 2) Separate out temperatures from horizontal and vertically drilled well bores. 3) Hire a well logging company to measure temperature through the full vertical portion of a shut in well, thus measuring equilibrium logs for calibration. 4) Model an updated correction curve for the various industries to use in calculating deeper temperatures.

Proposal: Thermal Conductivity Database

Maria Richards and Joseph Batir
SMU Geothermal Laboratory, Dallas, Texas

September 28, 2020

The Texas portion of the Heat Flow database in the National Geothermal Data System Node at SMU Geothermal Laboratory contains 33 rock measured thermal conductivity values, 56 thermal conductivity values reversed-calculated from published heat flow values, and the rest of the 16,384 heat flow values were derived from assigned (estimated) thermal conductivity values to derive a heat flow value. There are an additional 12,889 Bottom-hole temperature sites with assigned thermal conductivity values based on the Oklahoma Anadarko Basin analysis by Gallardo and Blackwell (1999). Combined, there are less than 100 rock measured thermal conductivity values for approximately 30,000 heat flow values. Texas heat flow maps and temperature-at-depth calculations are based on estimates and predicted correlations between basins.

The state of North Dakota used their core log library to improve their mapping of the Bakken play and the entire Williston Basin. In doing so, the thermal conductivity values differed within formations, at different depths, and locations (Gosnold et al., 2012; Crowell and Gosnold, 2013). Thus, the sedimentary settings and structure were more diverse than originally thought. For example, the Pierre Shale varied by ~10% and the Madison Limestone by ~15% with others varying even more (Figure 1).

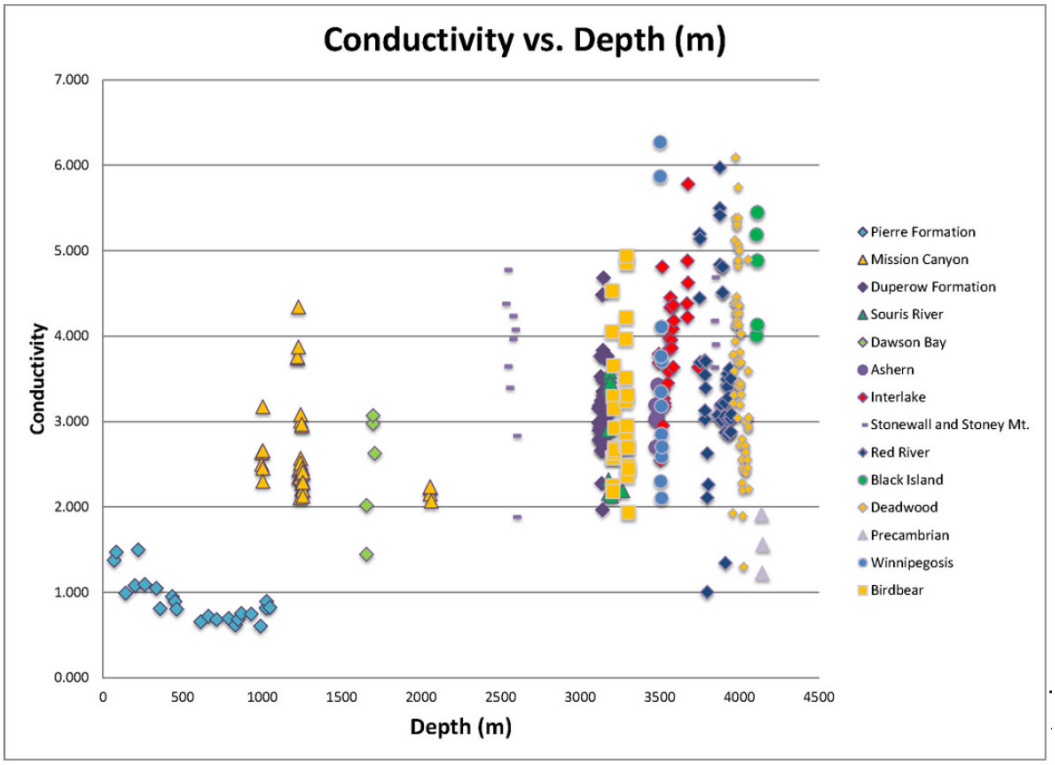

Figure 1. Thermal conductivity measured values (W/mK) versus depth of core sampled from the North Dakota Core Log Library. Work completed by Crowell and Gosnold (2013) and Gosnold et al., 2012

With the improved thermal conductivity values in the Williston Basin, the ability to correct bottom hole temperatures improved and the overall heat flow values increased. The work by Blackwell and Richards (2004) has a heat flow in the Williston Basin of 60-75 mW/m^2. The updated thermal conductivity values changed the heat flow values to 60-95 mW/m^2(Gosnold et al., 2012).

The SMU Geothermal Laboratory uses their divided bar to run samples for companies, government agencies, and students. The bar has been in use for over 40 years and considered one of the top labs for thermal conductivity analysis on cores and cuttings. The BEG Core Log Research Centers contain rock cores from across the state and throughout the formations. They are also able to drill plugs from the cores to prepare the samples for analysis. Therefore, working together SMU and BEG could develop a research program to improve the knowledge of thermal conductivity in Texas. This data would then be available to those in fossil fuels, geothermal energy, carbon sequestration, etc.,

Proposed Research

Review core log library for formation and depth then choose cores to be drilled for thermal conductivity measurements.

Run the samples and analyze the results.

Update Texas heat flow database with new measured values and correct the estimated values to be more consistent.

References

Blackwell, D.D. and Richards, M., 2004. Geothermal Map of North America: American Association of Petroleum Geologists. Tulsa, Oklahoma, scale (1: 6,500,000).

Crowell, J. and Gosnold, W.D., 2013. Detecting Spatial Trends in Thermal Conductivity in the Williston Basi. *GRC Transactions*, *37*(GRC1030612).

Gallardo, J. and Blackwell, D.D., 1999. Thermal structure of the Anadarko Basin. *AAPG bulletin*, *83*(2), pp.333-361.

Gosnold, W.D., McDonald, M.R., Klenner, R. and Merriam, D., 2012. Thermostratigraphy of the Williston Basin. *Transactions, Geothermal Resources Council*, *36*, pp.663-670.

Proposal: Combine Seismic Data and Heat Flow data to examine Radiogenic Heat Production

Maria Richards and Joseph Batir
SMU Geothermal Laboratory, Dallas, Texas

September 28, 2020

The oil and gas industry shows increasing interest in expanding their operations into the realm of geothermal energy resources. The success of the UT Austin GEO team's PIVOT conference in July 2020 is a current example along with the new Schlumberger business sector, Schlumberger New Energy, which signed an agreement in September 2020 with Thermal Energy Partners to develop geothermal energy projects.

This renews the importance of examining the Texas geothermal resources with improved techniques and data acquisition. The radiogenic heat production from deep sediments, basement, and even the mantle below Texas has rarely been studied. McKenna and Sharp (1998) did the lead assessment of the radiogenic heat production values from the sedimentary section focusing on South Texas. From this study they determined that deep sediments contributed up to 26% of the total surface heat flow and if heat production is not taken into consideration when extrapolating to deeper temperatures (6 km – 10 km) the deep temperatures are predicted to be too hot. The South Texas study shows radiogenic heat production values can vary by depth and within one formation, e.g., Wilcox Mudrock (.086 – 1.87 $\mu W/m^3$), Frio Sandstone (0.58 – 1.52 $\mu W/m^3$). This is one study using eight wells. The rest of Texas has even more limited measurements from core!

Radioactivity is still used in resources evaluation. Instead well logs, rather than physical core or cuttings, are used for the heat production values in use an assigned value to extrapolate through the sediment section of the basin for deep temperature calculations. With increased computing power and new heat production values, they could be used to improve these deep temperature calculations. Now is a time for additional accuracy for understanding our resources base and provide correct inputs for machine learning success.

From an improved radiogenic heat production database, there are multiple additional research opportunities. With increased understanding of the upper-sedimentary section contribution to the surface heat flow, the ability to examine of the deeper sediments and basement below Texas through models becomes applicable. Today the BEG collects seismic velocity data from sites within the TexNet Seismic Monitoring Program. This increase in seismic data provides increased resolution for working with seismic velocity profiles to calculate the deep radiogenic heat production (Cermak, Bodri, and Rybach, 1991). The results across Texas could improve the understanding of temperatures being extrapolated between 6 km and 10+ km as a second way to combine heat flow and heat production to calculate deep temperatures. Other research opportunities are the ability to examine possible fluid flow through deep faults, e.g., Balcones and Luling, and through geopressure exploration (Agrawal et al., 2015); use the velocity data to improve accuracy of the basement depth and lithosphere depth (Borgfeldt, 2017); and combine radiogenic heat production, seismic velocity, and heat flow to improve the time-temperature history of deep basins as highlighted by Mukerji et al., (2018).

Proposed Research

Work with the BEG Core Log Library to select cores/cuttings for radiogenic heat production analysis. Run the samples.

Collect and analyze seismic velocity profiles for detailed basement depth, and calculated radiogenic heat production for lithosphere through sediment within vicinity of core/cutting values.

Calculate new temperature-at-depth maps in higher resolution and with additional accuracy at values 6 km and deeper.

References

Agrawal, M., Pulliam, J., Sen, M.K. and Gurrola, H., 2015. Lithospheric structure of the Texas-Gulf of Mexico passive margin from surface wave dispersion and migrated Ps receiver functions. Geochemistry, Geophysics, Geosystems, 16(7), pp.2221-2239.

Borgfeldt, Taylor Marie, 2017, Crustal seismic velocity models of Texas, UT Austin MS thesis, Austin, Texas.

Čermák, V., Bodri, L. and Rybach, L., 1991. Radioactive heat production in the continental crust and its depth dependence. In Terrestrial Heat Flow and the Lithosphere Structure (pp. 23-69). Springer, Berlin, Heidelberg.

Mukerji, T., Dutta, N., Prasad, M. and Dvorkin, J., 2002. Seismic detection and estimation of overpressures. Part I: The rock physics basis: CSEG Recorder, 27, pp.34-57.